nature neuroscience

Article

https://doi.org/10.1038/s41593-022-01198-z

Neural basis of anticipation and premature impulsive action in the frontal cortex

Received: 25 March 2021

Accepted: 5 October 2022

Published online: 14 November 2022

Check for updates

Robertas Guzulaitis[1,2] ✉, Luca Godenzini[1] & Lucy Maree Palmer[1] ✉

Planning motor actions can improve behavioral performance; however, it can also lead to premature actions. Although the anterior lateral motor cortex (ALM) is known to be important for correct motor planning, it is currently unknown how it contributes to premature impulsive motor output. This was addressed using whole-cell voltage recordings from layer 2/3 pyramidal neurons within the ALM while mice performed a cued sensory association task. Here, a robust voltage response was evoked during the auditory cue, which was greater during incorrect premature behavior than during correct performance in the task. Optogenetically suppressing ALM during the cued sensory association task led to enhanced behavior, with fewer, and more delayed, premature responses and faster correct responses. Taken together, our findings extend the current known roles of the ALM, illustrating that ALM plays an important role in impulsive behavior by encoding and influencing premature motor output.

A primary function of the cortex is to process vast amounts of sensory information and execute appropriate motor programs. While some sensory inputs lead to direct actions, others serve as sensory cues that contribute to the planning of motor output. Sensory cues are thought to prime motor programming networks, changing neural activity in various brain circuits prior to behavioral output[1–8]. This priming of neural networks enhances behavior by improving performance and increasing behavioral speed[9,10]; however, sensory cues can also lead to anticipation and premature impulsive motor actions[11–15]. Since sensory cues influence behavioral performance, cued behavior needs to be controlled and constrained to achieve correct motor actions and optimal performance.

Impulsive actions are a form of anticipatory behavior that results from the inability to suppress inappropriate behaviors[12,15]. Such behavior can occur when greater importance is placed on immediate outcomes (that is, when speed is favored rather than accuracy) or simply from failure to stop automatic behaviors[12,15]. Waiting impulsivity is a form of impulsive behavior where a subject fails to wait until the appropriate time of action[16]. This leads to premature motor action and is associated with various modulatory systems[17] and brain regions[16,18,19].

Among many other functions[20], frontal cortex is involved in the acquisition and performance of skilled movements[21,22] and the ALM is specifically involved in the planning of such motor outputs[2–4,23]. Although the ALM contributes to motor planning, it is not clear how it influences impulsive behavior and premature motor actions. This is a vital piece of the puzzle which is necessary to understand the microcircuitry underlying motor planning since it involves, to some extent, the anticipation of motor output and often results in premature impulsive action. Here, we addressed this by establishing a cued sensory association task where mice demonstrated impulsive behavior. Using whole-cell patch-clamp recordings from layer 2/3 (L2/3) pyramidal neurons within the ALM and primary motor cortex (M1), we recorded the neural correlates of cue-triggered anticipation and used optogenetics to establish a causal link between the neural activity and premature impulsive behavior.

Results

Instructive cues shift the behavioral licking response

To investigate the neural basis of cued behavior, we trained mice to perform a cued sensory association task. Initially, mice were trained to receive a water reward if they licked a reward port within 1 s of receiving a tactile stimulus (200 Hz, 100 ms) delivered to the forepaw. Mice rapidly learnt this tactile association task, reaching expert performance (>80% HIT rate, sensitivity index (d′) > 1) within 2.94 ± 0.18 days (166 ± 4.64 Go trials daily, $n = 32$ mice; Extended Data Fig. 1). Once expert in the tactile association task, the tactile stimulus

[1]Florey Institute of Neuroscience and Mental Health, University of Melbourne, Melbourne, Victoria, Australia. [2]The Life Sciences Center, Vilnius University, Vilnius, Lithuania. ✉e-mail: robertas.guzulaitis@gmc.vu.lt; lucy.palmer@florey.edu.au

https://doi.org/10.1038/s41593-022-01198-z

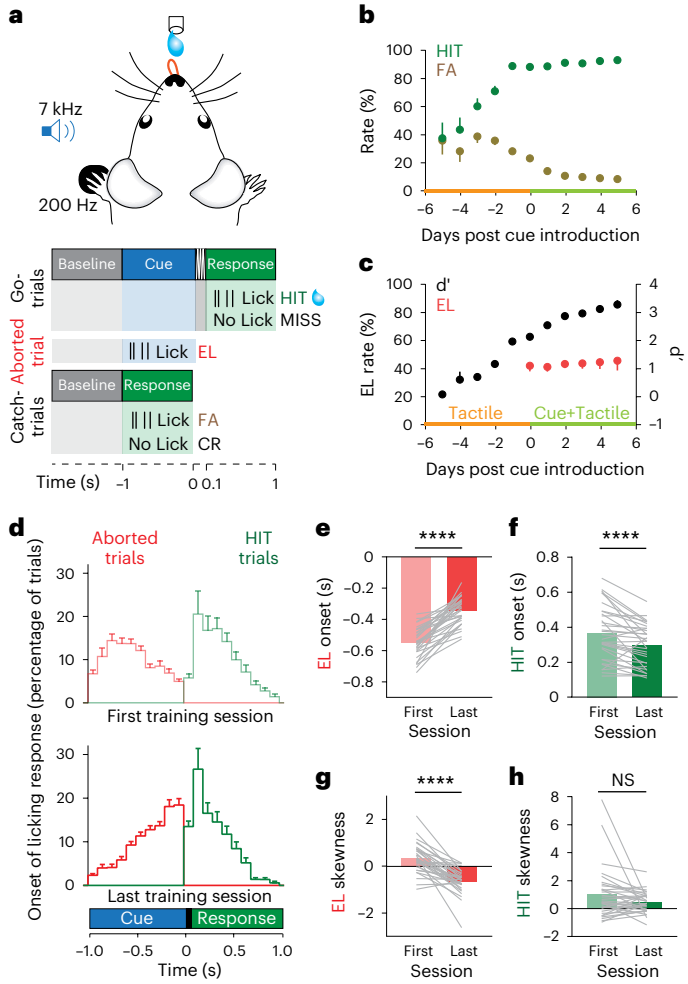

Fig. 1 | Instructive cues shift the behavioral licking response in a cued sensory association task. a, The cued sensory association task design. An auditory cue (1 s, 7 kHz, 60 dB) was followed by tactile stimulation (200 Hz, 0.1 s). To receive a water reward (5–10 µl, 10% sucrose), mice were trained to lick a water port up to 1 s after the tactile stimulation (HIT). If mice did not lick the water port during the trial, it was classified as a MISS trial. Trials were aborted if mice licked the water port during the auditory cue (ELs). Go trials were randomly interleaved with Catch trials where no stimulus was delivered and the mice should not respond (correct rejection (CR)). If mice licked the water port during a Catch trial, it was classified as a false alarm (FA). **b**, Behavioral performance before (orange) and after (green) the introduction of the auditory cue in the cued sensory association task for correct behavior (HIT; green) and incorrect spontaneous licking during Catch trials (FA; fawn) ($n = 32$ mice). Data are presented as mean ± s.e.m. **c**, The d′ and EL rates throughout training before (orange) and after (green) the introduction of the auditory cue in the sensory association task ($n = 32$ mice). Data are presented as mean ± s.e.m. **d**, Distribution of the onset of the first lick for HIT (green) and EL (red) trials during the first (top) and last training sessions (bottom) ($n = 32$ mice). Data are presented as mean ± s.e.m. **e**, The average onset of the licking response in EL trials during the first and last training sessions in the cued sensory association task ($P < 0.0001$, two-tailed Wilcoxon test, $n = 32$ mice). Onset was measured from the end of the auditory cue. **f**, The average onset of the licking response in HIT trials during the first and last training sessions in the cued sensory association task ($P < 0.0001$, two-tailed Wilcoxon test, $n = 32$ mice). Onset was measured from the end of the auditory cue. **g**, Skewness of the distribution of lick latencies during EL trials during the first and last training sessions in the cued sensory association task ($P < 0.0001$, two-tailed Wilcoxon test, $n = 32$ mice). **h**, Skewness of the distribution of lick latencies during HIT trials during the first and last training sessions in the cued sensory association task ($P = 0.14$, two-tailed Wilcoxon test, $n = 32$ mice). Not significant (NS), $P > 0.05$; ****$P < 0.0001$.

was then preceded by an instructive auditory cue (7 kHz, 60 dB, 1 s). In this cued sensory association task, mice were still rewarded if they correctly responded by licking the reward port within 1 s after receiving the tactile stimulus; however, trials were aborted and mice did not receive the water reward if they responded during the auditory cue (early-lick (EL); Fig. 1a). Following the introduction of the instructive auditory cue to the sensory association task, mice were trained for a further 5.25 ± 0.21 d (256.07 ± 15.64 trials daily; $n = 32$ mice). Overall, training in the cued sensory association task led to further improvement in task performance, including a significant increase in HIT rate from 88.97 ± 1.17% to 93.92 ± 1.04% ($P < 0.0001$, $n = 32$ mice; Fig. 1b and Extended Data Fig. 2a), decrease in false alarm rate from 23.49 ± 2.65% to 7.94 ± 0.90% ($P < 0.0001$, $n = 32$ mice; Fig. 1b and Extended Data Fig. 2b) and increase in d′ from 2.11 ± 0.10 to 3.27 ± 0.10 ($P < 0.0001$, $n = 32$ mice; Fig. 1c and Extended Data Fig. 2c). Despite these improvements, the EL rate was not altered during subsequent sessions in the cued sensory association task, with an average rate of 41.48 ± 4.02% in the first session and 41.76 ± 3.41% in the last session ($P = 0.82$, $n = 32$ mice; Fig. 1c and Extended Data Fig. 2d). Next, characteristics of the licking response were investigated during both rewarded (HIT) and aborted (EL) trials (Supplementary Fig. 1). Although the rate of trials aborted due to impulsive behavior did not change throughout the cued sensory association task, the timing and pattern of these premature ELs did (Fig. 1d). Following training, the auditory cue shifted the onset of the average EL response closer to the presentation of the tactile stimulus (from −0.55 ± 0.02 s to −0.34 ± 0.02 s; $P < 0.0001$, $n = 32$ mice; Fig. 1e). Likewise, the average onset of the licking response during HIT trials was also shifted by the auditory cue, with significantly slower response times to the tactile stimulus in the first session (0.37 ± 0.03 s) compared with the last session (0.30 ± 0.02 s; $P < 0.0001$, $n = 32$ mice; Fig. 1f). This change in the onset of the licking response during the cued sensory association task is further illustrated by the change in the distribution of the licking onset during the auditory cue, which was positively skewed during the first session (0.36 ± 0.11) and negatively skewed during the last session (−0.65 ± 0.09; $P < 0.0001$, $n = 32$ mice; Fig. 1g). In contrast, the distribution of licking responses during HIT behavior was not significantly different throughout training in the cued sensory association task (first session, 1.03 ± 0.33; last session, 0.45 ± 0.13; $P = 0.14$, $n = 32$; Fig. 1h).

To test whether the changed licking behavior during the cued sensory association task was indeed due to the introduction of the instructive cue and not the additional training, mice expert in the cued sensory association task were presented with the tactile stimulus either with (cued) or without (non-cued) the auditory cue (Extended Data Fig. 3). Here, the cued trials had a significantly faster response time compared with non-cued trials during HIT behavior (0.12 ± 0.01 s versus 0.16 ± 0.01 s; $P = 0.03$, $n = 6$ mice), illustrating that the auditory cue, and not additional training, leads to changes in licking behavior. To further investigate the influence of the instructive cue on behavior, we next investigated whether mice rely on the learnt duration of the cue to successfully perform the task. Here, varying cue duration altered both the rate and timing of the licking response in EL trials (Extended Data Fig. 4a–c) but not HIT trials (Extended Data Fig. 4d,e), suggesting that mice were, at least partially, relying on the timing of the instructive cue. Furthermore, omission of the tactile stimulus following the instructive cue led to a significant decrease in the task performance, decreasing HIT rate (94.98 ± 2.72% versus 64.13 ± 4.81%; $P = 0.03$, $n = 6$ mice) and increasing response time (0.12 ± 0.01 s versus 0.19 ± 0.03 s; $P = 0.03$, $n = 6$ mice; Extended Data Fig. 5), illustrating that the performance in the cued sensory association task also required the tactile stimulus. Together, these findings illustrate that mice performing the cued sensory association task use both the instructive auditory cue and the tactile stimulus.

Changes in licking behavior following training in the cued sensory association task suggests that mice learn to use the instructive auditory

cue to predict the reward epoch, leading to changes in the timing of the behavioral response. Despite greater overall performance in the task, the EL rate was constant during training in the cued sensory association task, illustrating that premature licking behavior was refined, but not decreased, by training.

ALM neurons have a robust voltage response during the cue

Since the auditory cue influenced the overall performance in the cued sensory association task, we assessed the level of arousal during the cue by recording the dynamic changes in pupil diameter[24,25] in both expert and naïve mice (Fig. 2a). In expert mice, there was a significant increase in pupil dilation from baseline during the auditory cue (4.65 ± 1.44%; $P = 0.002$, $n = 10$ mice; Fig. 2b). Although pupil dilation was greatest during the reward delivery, the increase in pupil dilation during the cue suggests that expert mice are attending to the cue. This was further illustrated by a significant increase in pupil dilation throughout training in the cued sensory association task ($P = 0.037$, $n = 10$ mice; Supplementary Fig. 2). In contrast, there was no significant change in pupil diameter during presentation of the auditory cue in naïve mice ($P = 0.12$, $n = 11$ mice; Fig. 2c). These findings suggest that mice were aroused by the sensory cue only after it was associated with a positive reward during expert performance in the cued sensory association task ($P = 0.005$, $n = 10$ expert/11 naïve mice; Fig. 2d).

Next, due to the influence of the instructive cue on arousal and impulsive behavior, we investigated the neural activity underlying the cued behavior. Since the ALM is known to be involved in motor planning[3,4], we performed whole-cell patch-clamp recordings from L2/3 pyramidal neurons within the ALM while mice performed the cued sensory association task (average somatic depth below pia, 290 ± 17 µm; $n = 16$ neurons; Fig. 2e). Using this approach, neural activity could be correlated with the corresponding behavioral licking response (Fig. 2f). During correct performance (HIT trials), a robust voltage response was evoked during the auditory cue (4.02 ± 0.73 mV from baseline voltage of −52.59 ± 2.84 mV; $P = 0.0001$, $n = 14$ neurons, 4 mice; Fig. 2g,h and Extended Data Fig. 6a,b), leading to a twofold increase in action potential firing rate (1.34 ± 0.56 Hz to 2.61 ± 1 Hz; $P = 0.03$, $n = 10$ neurons, 4 mice; Fig. 2h). The onset of this voltage response occurred during the auditory cue (−867.9 ± 11.36 ms before tactile stimulus), which was over a second before the average onset of the licking behavior (343.91 ± 43.46 ms after the tactile stimulus; $P = 0.004$, $n = 9$ neurons, 4 mice; Extended Data Fig. 6c,d). Therefore, the temporal disconnect between the voltage and behavior suggests that the voltage response during HIT trials was not due to the licking behavior itself. The voltage response was also not due to the encoding of sensory (auditory and/or tactile) information, as in contrast to expert mice, the sensory stimuli (auditory cue followed by tactile) did not evoke a detectable voltage response in naïve mice (Fig. 2i). Here, there was no change in the membrane potential (−0.001 ± 0.15 mV from resting voltage of −59.8 ± 1.8 mV; $P = 0.92$, $n = 21$ neurons, 3 mice) or the action potential firing rate (baseline, 1.18 ± 0.64 Hz versus Cue, 1.15 ± 0.63 Hz; $P = 0.25$, $n = 8$ neurons, 3 mice; Fig. 2j) during the auditory cue in awake naïve mice. This suggests that, similar to arousal, the activity of L2/3 pyramidal neurons within the ALM is context dependent as sensory information is typically not encoded unless it is salient and associated with a reward or action.

Enhanced response in ALM neurons during correct performance

Is the neuronal activity evoked during the cued sensory association task correlated with task performance? To test this, we investigated the small (<10%) subset of trials where, despite expert performance, mice did not respond (MISS; Fig. 3a). During these unrewarded MISS trials, mice were still aroused by the auditory cue, as illustrated by a significant increase in pupil dilation above baseline (by 3.7 ± 1.3%; $P = 0.04$, $n = 8$ mice) which was similar to HIT trials ($P = 0.97$, $n = 10/8$ mice; Fig. 3b). Therefore, even though the mice did not actively respond in MISS trials, the similar pupil dynamics suggest that mice were equally aroused during the auditory cue irrespective of the trial outcome. We next assessed whether L2/3 pyramidal neurons within the ALM were also active in MISS trials (Fig. 3c). During MISS trials, the auditory cue evoked a small voltage response that was on average 0.91 ± 0.32 mV in amplitude ($P = 0.031$, $n = 6$ neurons, 4 mice; Fig. 3d). Despite similar states of arousal, this cue-evoked voltage response during MISS trials was significantly smaller in amplitude than the voltage response during HIT trials ($P = 0.033$, $n = 6/14$ neurons during MISS/HIT trials; Fig. 3e,f) and returned to baseline before the end of the cue (0.43 ± 0.37 mV; $P = 0.44$, Wilcoxon test, $n = 6$ neurons, 4 mice; Extended Data Fig. 7c). This is in contrast to HIT trials, where the voltage response significantly increased throughout the auditory cue (3.13 ± 0.56 mV to 4.92 ± 0.91 mV; $P = 0.0002$, $n = 14$ neurons, 4 mice; Extended Data Fig. 7b). Taken together, these results suggest that the instructive auditory cue evokes a prolonged voltage response in ALM neurons during HIT trials that far exceeds the sensory or arousal response, and may encode behaviorally relevant anticipatory information for priming motor output.

M1 neurons have a small voltage response during the cue

Is the voltage response during the cued sensory association task specific to ALM neurons? To test this, we performed whole-cell patch-clamp recordings from L2/3 pyramidal neurons within a neighboring cortical region also known to be involved in sensory association tasks, the primary motor cortex (M1; Fig. 4a). In these recordings, behavioral performance was similar to mice where recordings were performed from ALM. During HIT performance in the cued sensory association task, the average amplitude of the voltage response in M1 neurons during the auditory cue was 1.18 ± 0.29 mV ($n = 20$ neurons, 6 mice; Fig. 4b). In contrast to the large and rapid depolarization at the onset of the auditory cue in ALM neurons during HIT trials, M1 neurons had a slow ramping depolarization throughout the cue (Fig. 4b) which was significantly smaller in amplitude than ALM neurons ($P = 0.0007$, $n = 20/14$ neurons; Fig. 4c,d). Furthermore, no detectable voltage response to the auditory cue in MISS trials was recorded in M1 neurons, in contrast to the discernible cue-evoked voltage response in ALM neurons ($P = 0.018$, $n = 12/6$ neurons; Fig. 4e,f). These differences between L2/3 pyramidal neurons within ALM and M1 illustrate that instructive cues are not universally encoded throughout the cortex, and suggest that the ALM may play a unique role during cued behavior.

ALM neurons have increased voltage during impulsive behavior

Despite expert performance in the cued sensory association task, mice prematurely licked the water port during the auditory cue in about 40% of trials (Fig. 1c and Extended Data Fig. 2d). These premature EL trials were aborted following the first incorrect lick and no water reward was delivered (Fig. 5a). To determine whether the ALM is also active during premature behavior, we assessed the voltage response in L2/3 pyramidal neurons within ALM during these aborted EL trials (Fig. 5b,c). Here, neurons had a large voltage response during the auditory cue (5.81 ± 0.72 mV from baseline voltage of −52.5 ± 2.41 mV; $P = 0.0002$, $n = 13$ neurons, 4 mice; Fig. 5d) which led to an approximate threefold increase in action potential firing above baseline (1.16 ± 0.55 Hz versus 3.3 ± 1.08 Hz; $P = 0.004$, $n = 9$ neurons, 4 mice; Fig. 5e). Similar to HIT trials, this voltage response during EL trials in ALM neurons was not simply due to licking itself as the onset of the voltage response occurred well before the behavioral licking response (lick onset, −220.2 ± 26.84 ms; voltage onset, −881.6 ± 11.94 ms; $P = 0.001$, $n = 11$ neurons, 4 mice; Supplementary Fig. 3) and the voltage response during premature EL behavior was significantly larger in neurons within ALM compared with M1 (M1, 3.37 ± 0.72 mV; $P = 0.02$, two-tailed Mann–Whitney test, $n = 12$ neurons, 6 mice). Combined with the large cue-evoked voltage

https://doi.org/10.1038/s41593-022-01198-z

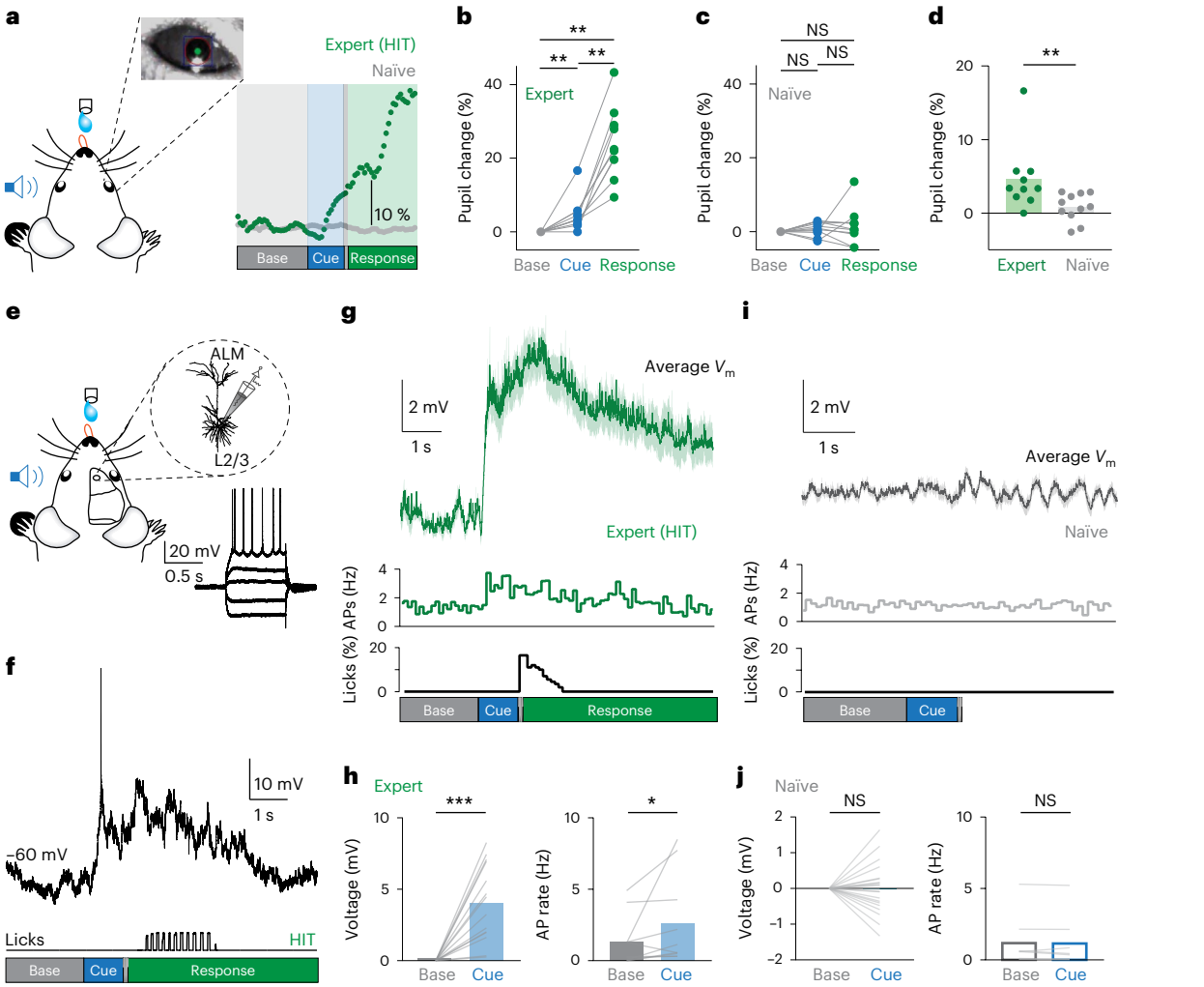

Fig. 2 | ALM neurons have a robust voltage response during the auditory cue in expert mice. a, Pupil tracking experimental design. Typical example of the average pupil dilation during the sensory stimulus (auditory cue, 1 s, 7 kHz, 60 dB followed by tactile stimulation, 200 Hz, 0.1 s) in a naïve mouse (gray) and an expert mouse performing the cued sensory association task (HIT; green). **b**, Average change in the pupil diameter during baseline (1 s before cue), cue (0.5–1.0 s post onset) and response (0.5–2 s post tactile stimulus) in expert mice correctly performing the cued sensory association task (HIT; baseline versus cue, $P = 0.002$; baseline versus response, $P = 0.002$; cue versus response, $P = 0.002$; two-tailed Wilcoxon test, $n = 10$ mice). **c**, Average change in the pupil diameter in naïve mice that were presented with the sensory stimulus (auditory cue followed by tactile stimulation) used in the cued sensory association task (naïve; baseline versus cue, $P = 0.12$; baseline versus response, $P = 0.46$; cue versus response, $P = 0.37$; two-tailed Wilcoxon test, $n = 11$ mice). **d**, Change in the average pupil diameter during the auditory cue in expert mice correctly performing the cued sensory association task (green) and naïve mice (gray) ($P = 0.005$, two-tailed Mann–Whitney test, $n = 10$ expert/11 naïve mice). **e**, Experimental design. Whole-cell patch-clamp recordings were performed from L2/3 pyramidal neurons within ALM (AP 2.5, ML 1.5 from bregma) in naïve and expert mice performing the cued sensory association task. Inset, voltage response to 50-pA current step. **f**, An example voltage recording (top) and licking response (bottom) during a HIT trial. **g**, Grand average (dark green) and standard error (light green) voltage response (top), mean firing rate (middle) and licking behavior (bottom) for all recorded L2/3 pyramidal neurons during correct performance (HIT trials) in the cued sensory association task. Licks, proportion of trials where the first lick response occurred. **h**, Average voltage response amplitude ($n = 14$ neurons, 4 mice; left) and action potential rate ($n = 10$ neurons, 4 mice; right) during baseline (gray) and the auditory cue (blue) during correct performance (HIT trials) in expert mice (voltage, $P = 0.0001$, two-tailed Wilcoxon test, $n = 14$ neurons, 4 mice; action potential rate, $P = 0.03$, two-tailed Wilcoxon test, $n = 10$ neurons, 4 mice). **i**, Grand average (dark gray) and standard error (light gray) voltage response (top), mean firing rate (middle) and licking behavior (bottom) for all recorded L2/3 pyramidal neurons in naïve mice presented with the sensory stimulus (auditory cue followed by tactile stimulation). **j**, Average voltage response amplitude ($n = 21$ neurons, 3 mice; left) and action potential rate ($n = 8$ neurons, 3 mice; right) during baseline (gray) and the auditory cue (blue) in naïve mice presented with the sensory stimulus (auditory cue followed by tactile stimulation) (voltage, $P = 0.92$, two-tailed Wilcoxon test, $n = 21$ neurons, 3 mice; action potential rate, $P = 0.25$, two-tailed Wilcoxon test, $n = 8$ neurons, 3 mice). NS, $P > 0.05$; *$P < 0.05$; **$P < 0.01$; ***$P < 0.001$.

response during correct behavior, these results further illustrate that ALM neurons prominently encode instructive cues.

Our findings illustrate that auditory cues evoke a large voltage response in ALM neurons during both correct and premature behavior. Does this cue-evoked voltage response differ according to the behavioral outcome? To test this, we directly compared the voltage responses in HIT and EL trials (Fig. 6a). Here, the onset of the licking response was significantly different between HIT and EL trials (relative to tactile stimulus, HIT, 324.7 ± 44.22 ms; EL, −198 ± 33.8 ms; $P = 0.008$, $n = 8$ neurons, 4 mice; Fig. 6b). However, in contrast to the licking behavior, the onset of voltage response in L2/3 neurons in ALM did not differ according to behavioral outcome (HIT, −870.3 ± 12.6 ms; EL, −897.1 ± 10.84 ms; $P = 0.11$, $n = 8$ neurons, 4 mice; Fig. 6b). This disconnect between the onset of the cue-evoked voltage response and the

https://doi.org/10.1038/s41593-022-01198-z

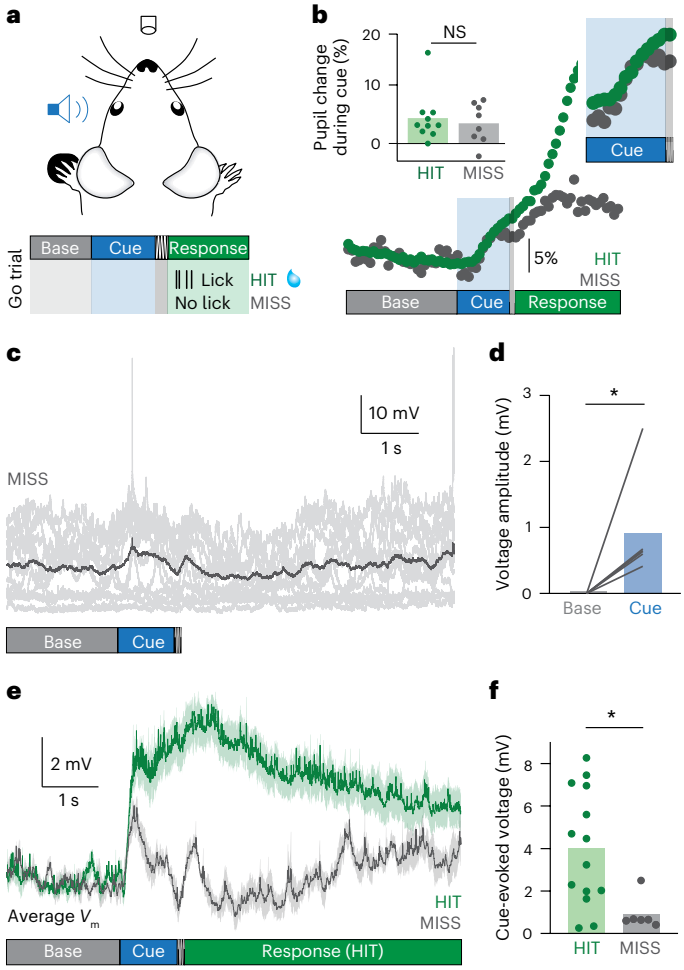

Fig. 3 | ALM neurons have an enhanced voltage response to the auditory cue during correct performance. a, During the cued sensory association task, expert mice received a water reward if they licked the water port up to 1 s after the auditory cue (HIT). Mice did not receive a water reward if they did not lick the water port during the trial (MISS). **b**, Grand average pupil dilation during HIT and MISS trials. Inserts, similar pupil dilation during the auditory cue was observed during both HIT and MISS trials ($P = 0.97$, two-tailed Mann–Whitney test, $n = 10/8$ mice for HIT/MISS trails). **c**, Overlay of individual (light gray) and grand average (dark gray) voltage responses during MISS trials in an example recorded L2/3 pyramidal neuron in ALM. **d**, Average voltage response amplitude in MISS trials during the auditory cue compared with the baseline ($P = 0.031$, two-tailed Wilcoxon test, $n = 6$ neurons, 4 mice). **e**, Grand average (dark color) and standard error (light color) voltage response for all recorded L2/3 pyramidal neurons during HIT (green) and MISS (gray) trials in the cued sensory association task. **f**, Average amplitude of the voltage response in HIT (green) and MISS (gray) trials during the auditory cue ($P = 0.033$, two-tailed Mann–Whitney test, $n = 14/6$ neurons for HIT/MISS trails). NS, $P > 0.05$; *$P < 0.05$.

onset of the licking behavior again demonstrates that the onset of the voltage response in L2/3 pyramidal neurons is not directly determined by the motor action.

To directly compare the amplitude of the cue-evoked voltage response, we needed to assess the voltage response without the confound of licking behavior. We therefore compared the voltage response evoked before the onset of the licking response in both HIT and EL trials (0–0.5 s after cue onset; Fig. 6a). Here, the voltage response evoked during the auditory cue was significantly larger in EL trials (4.76 ± 0.73 mV) compared with HIT trials (3.49 ± 0.64 mV; $P = 0.001$, $n = 11$ neurons, 4 mice; Fig. 6c). Similarly, accounting for any voltage within the ALM associated with the execution of the licking motion[26] and reaction time to the stimulus (Extended Data Fig. 3), a briefer time window of analysis (0–0.3 s after cue onset) also resulted in a significantly larger voltage response during EL trials compared with HIT trials (3.78 ± 0.44 mV versus 2.48 ± 0.48 mV; $P = 0.007$, two-tailed Wilcoxon test, $n = 11$ neurons, 4 mice). In a subset of mice, nuchal electromyogram (EMG) recordings were performed during the voltage recordings to identify if there was increased gross motor activity in EL trials which could be linked to greater voltage responses (Extended Data Fig. 8a,b). Overall, there was no measurable difference in EMG activity between HIT and EL trials ($P = 0.47$, $n = 7$ sessions, 3 mice; Extended Data Fig. 8c), suggesting that differences in voltage were not due to measurable differences in body motion. Therefore, in the absence of motor behavior, incorrect EL trials had a larger voltage response during the auditory cue in ALM neurons. Interestingly, although the average resting membrane potential during the HIT and EL trials was similar ($P = 0.64$, two-tailed Wilcoxon test, $n = 11$ neurons, 4 mice), there was a gradual ramping of the voltage before the onset of the auditory cue in EL trials (1.55 ± 0.55 mV s^{-1}; $P = 0.02$, $n = 11$ neurons, 4 mice) but not in HIT trials (0.51 ± 0.56 mV s^{-1}; $P = 0.46$, $n = 11$ neurons, 4 mice; Fig. 6d,e). This gradual voltage ramp during EL trials led to a more depolarized voltage before the auditory cue onset (by 0.96 ± 0.31 mV; $P = 0.02$, $n = 11$ neurons, 4 mice; Extended Data Fig. 9a,b). In contrast, the voltage before the auditory cue onset during HIT trials was not depolarized (0.26 ± 0.23 mV; $P = 0.32$, $n = 11$ neurons, 4 mice; Extended Data Fig. 9c). Therefore, L2/3 pyramidal neurons within ALM had increased voltage activity before, and during, the auditory cue in trials where mice displayed impulsive premature behavior.

Suppression of ALM reduces impulsive premature behavior

To test if there is a causal link between the activity of L2/3 pyramidal neurons within the ALM and the cued sensory association behavior, we performed optogenetic inactivation of the ALM while mice were performing the cued sensory association task. Here, transgenic PV^+ (parvalbumin) Cre mice were injected with the excitatory opsin (pAAV-EF 1a-doublefloxed-hChR2(H134R)-EYFP-WPRE-HGHpA) bilaterally into the ALM (Methods). First, we assessed whether photo-activation of ChR2-expressing PV interneurons in the ALM led to inhibition of principal neurons within the ALM injection site. Whole-cell patch-clamp recordings were performed from L2/3 pyramidal neurons within the ALM during a train of brief (10-ms) light-emitting diode (LED) pulses (470 nm, 2–5 mW; 40 Hz, 1 s) onto the cortical surface in anesthetized mice (Fig. 7a). Here, photo-activation of PV interneurons within ALM caused hyperpolarization (by 3.25 ± 1.02 mV from baseline; $P = 0.004$, $n = 21$ neurons, 5 mice; Fig. 7b,c) and abolished the spontaneous firing rate (from 2.02 ± 0.49 to 0.18 ± 0.1 Hz; $P < 0.0001$, $n = 21$ neurons, 5 mice; Fig. 7d) in L2/3 pyramidal neurons within the ALM. Cessation of the photo-activation of PV interneurons led to a return of spiking to the resting firing rates in ALM pyramidal neurons (2.22 ± 0.53 Hz; $P = 0.29$, $n = 21$ neurons, 5 mice; Extended Data Fig. 10). Next, we tested the influence of photo-inhibiting the ALM on the behavioral performance in the cued sensory association task. Fiber optics were implanted bilaterally above the ALM cortex in transgenic PV^+ Cre mice that were previously injected with ChR2 into the ALM of both hemispheres (Fig. 7e,f). Mice were then trained in the cued sensory association task. Once expert in the task, LED pulses were delivered to the ALM during the auditory cue in half of the randomly interleaved trials (Fig. 7g). There was no difference in HIT rates between non-LED trials (97.27 ± 0.88%) and trials when the ALM was photo-inhibited (LED ON; 98.31 ± 0.45%; $P = 0.44$, $n = 6$ mice; Fig. 7h). In contrast, photo-inhibition of the ALM significantly decreased the number of trials aborted due to premature licking (LED ON, 33.82 ± 8.76%; LED OFF, 42.95 ± 9.26%; $P = 0.03$, $n = 6$ mice; Fig. 7h). ALM photo-inhibition was performed over 3 consecutive days, with no significant difference in behavior between test days ($P = 0.43$, Friedman analysis of variance (ANOVA), $n = 6$ mice). We next assessed the influence of ALM photo-inhibition during the auditory cue on the timing

https://doi.org/10.1038/s41593-022-01198-z

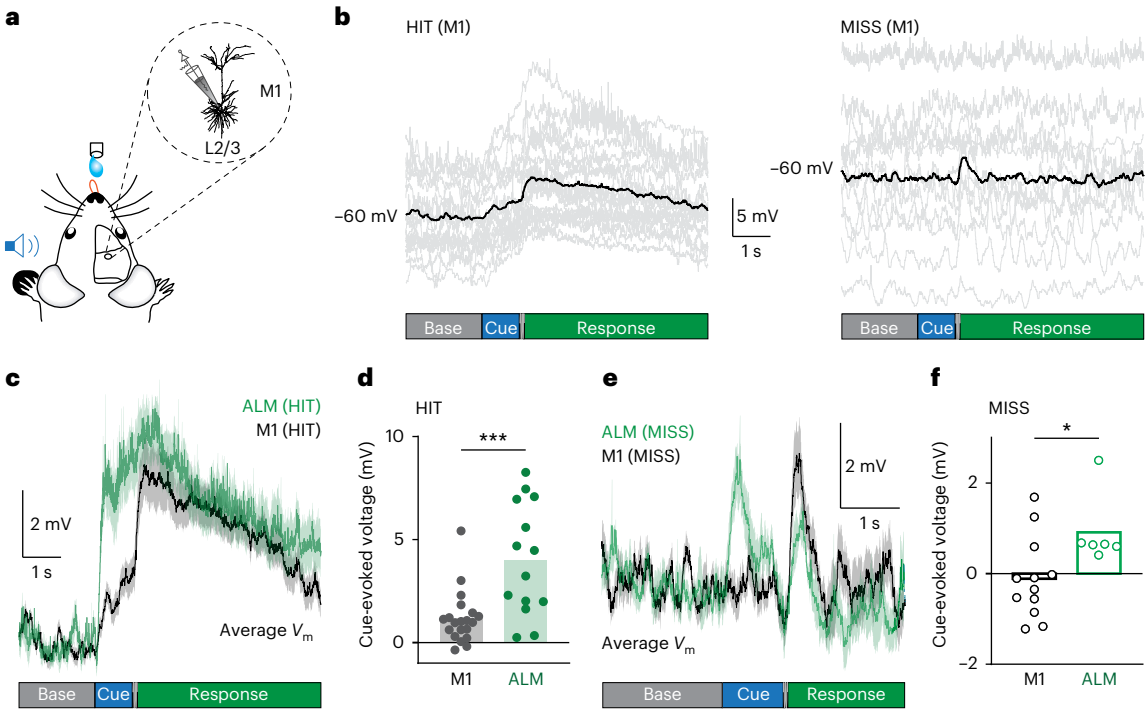

Fig. 4 | M1 neurons have a small voltage response to the instructive auditory cue during the cued sensory association task. a, Experimental design. Whole-cell patch-clamp recordings were performed from L2/3 pyramidal neurons within M1 (AP 0.25, ML 1.5 from bregma) in expert mice performing the cued sensory association task. **b**, Overlaid average voltage responses of recorded neurons (light gray) and grand average (black) during HIT (left) and MISS (right) trials of all recorded L2/3 pyramidal neurons in M1. **c**, Grand average (dark color trace) and standard error (light color shading) voltage response of all recorded L2/3 neurons in M1 (black) and ALM (green) during correct performance (HIT trials) in the cued sensory association task. **d**, Average voltage response of L2/3 neurons from M1 (gray; $n = 20$ neurons, 6 mice) and ALM (green; $n = 14$ neurons, 4 mice) during the auditory cue during HIT trials ($P = 0.0007$, two-tailed Mann–Whitney test). **e**, Grand average (dark color trace) and standard error (light color trace) voltage response of all recorded L2/3 neurons in M1 (black) and ALM (green) during MISS trials. **f**, Average voltage response of L2/3 neurons from M1 (black; $n = 12$ neurons, 5 mice) and ALM (green; $n = 6$ neurons, 4 mice) during the auditory cue during MISS trials ($P = 0.018$, two-tailed Mann–Whitney test). $^*P < 0.05$; $^{***}P < 0.001$.

of the behavioral response (latency to first lick). Despite no difference in the HIT rate, there was a significant decrease in the latency to the first lick when the ALM was photo-inhibited during the auditory cue (LED ON, 204.7 ± 19.35 ms; LED OFF, 232.8 ± 27.99 ms; $P = 0.03$, $n = 6$ mice; Fig. 7i). Photo-inhibition of the ALM also significantly altered the average lick latency in the EL trials, with mice licking later during the auditory cue (LED ON, −222.3 ± 22.31 ms; LED OFF, −283.2 ± 32.13 ms; $P = 0.03$, $n = 6$ mice; Fig. 7i). Overall, photo-inhibition of ALM during the auditory cue had the greatest influence on EL behavior compared with HIT behavior, with a greater effect on the evoked rate (−9.13 ± 0.83% versus 1.04 ± 0.77%; $P = 0.03$, $n = 6$ mice; Fig. 7j) and latency to the first lick response (60.92 ± 14.58 ms versus −28.05 ± 9.11 ms; $P = 0.03$, $n = 6$ mice; Fig. 7k) during EL trials. In contrast, in control mice injected with a non-light-sensitive GFP (AAV1/2-muGFP), there was no significant difference in the evoked rates (HIT, 90.89 ± 2.82 versus 90.03 ± 3.11; $P = 0.44$; EL, 44.66 ± 9.64% versus 44.31 ± 10.11%; $P = 0.84$; Fig. 7l) or latency to the first lick response (HIT, 296 ± 39.86 ms versus 292.5 ± 39.84 ms; $P = 0.56$; EL, −383.2 ± 38.14 ms versus −391.2 ± 38.86 ms; $P = 0.22$; $n = 6$ mice; Fig. 7m) in LED ON and LED OFF trials. Furthermore, photo-inhibition during the reward window in PV^+ Cre mice that were previously injected with ChR2 into the ALM of both hemispheres ($n = 6$ mice; Fig. 7g) also had no significant influence on either the behavior rate (HIT, $P = 0.31$; EL, $P = 0.69$; Fig. 7n) or lick latency (HIT, $P = 0.99$; EL, $P = 0.31$; Fig. 7o).

Taken together, these results suggest that the ALM predominantly influences premature licking during the auditory cue in the cued sensory association task. Silencing the ALM during the instructive auditory cue enabled expert mice to decrease premature licking, improving the overall performance in the cued sensory association task.

Discussion

In a process often referred to as 'impulsive control', learnt motor behavior requires both motor action and the inhibition of premature responses. Previous studies have highlighted the role of ALM in correct motor planning, but its role in impulsive control is largely unknown. In this study, we demonstrate that the ALM plays an important role in impulsive behavior, with enhanced voltage responses during instructive cues that lead to increased premature cue-evoked behavior.

Previous studies have typically focused on the function and role of the ALM during motor planning and correct motor output[27]. Although these studies often exclude trials in which premature actions are present, overall, our findings are in agreement with the role of the ALM in motor planning and correct motor output. We illustrate that the ALM encodes sensory cues during trials with motor output. However, our findings further suggest that the ALM is encoding more than motor output as (1) the voltage response was significantly greater during premature behavior despite similar motor output during correct behavior, (2) there was no correlation between motor output and voltage onset during the different behavioral outcomes and (3) photo-inhibition of the ALM had a greater influence on premature impulsive behavior. Therefore, our study adds to the growing repertoire of the functional roles performed by the frontal cortex[20] which has expanded to now include encoding and influencing premature impulsive behavior.

Although the onset of the voltage response in ALM neurons occurred during the auditory cue in both correct and premature behavior, this evoked voltage does not simply represent direct sensory encoding as pyramidal neurons were not responsive to the auditory cue in naïve mice. The experience-dependent voltage response may

https://doi.org/10.1038/s41593-022-01198-z

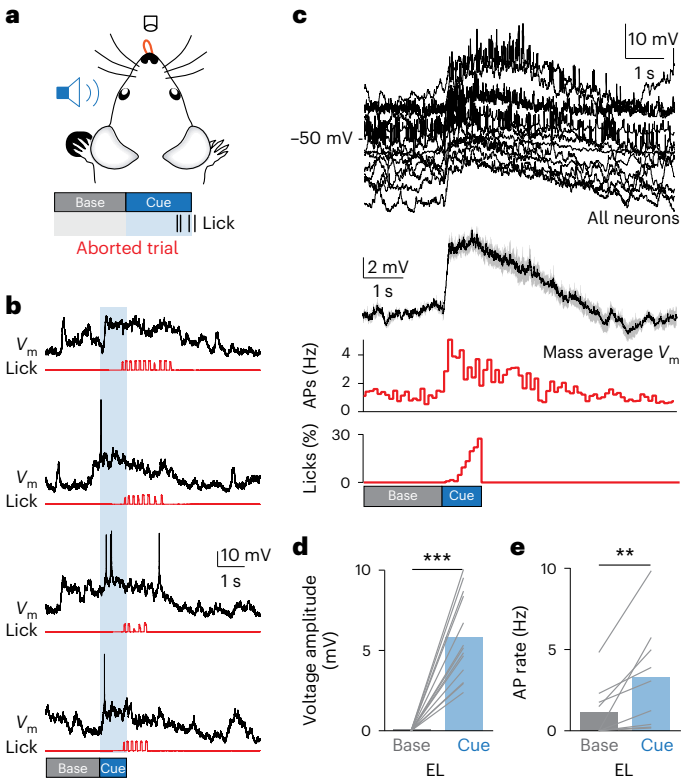

Fig. 5 | ALM neurons have a large voltage response during impulsive premature behavior. a, Trials were aborted and no reward was delivered if mice licked during the auditory cue in the cued sensory association task. **b**, Somatic voltage (black) and associated licking response (red) for an example L2/3 pyramidal neuron. Behavioral protocol is shown at the bottom. **c**, Overlaid average voltage responses of all recorded neurons (top) and grand average (black) and standard error (gray) voltage response (middle), mean firing rate and licking response (bottom) for all recorded L2/3 pyramidal neurons during EL trials in the cued sensory association task. Licks, proportion of trials where the first lick response occurred. **d**, Amplitude of the voltage response in EL trials during the auditory cue zeroed to baseline ($P = 0.0002$, two-tailed Wilcoxon test, $n = 13$ neurons, 4 mice). **e**, Firing rate during baseline and auditory cue in EL trials ($P = 0.004$, two-tailed Wilcoxon test, $n = 9$ neurons, 4 mice). $^{**}P < 0.01$; $^{***}P < 0.001$.

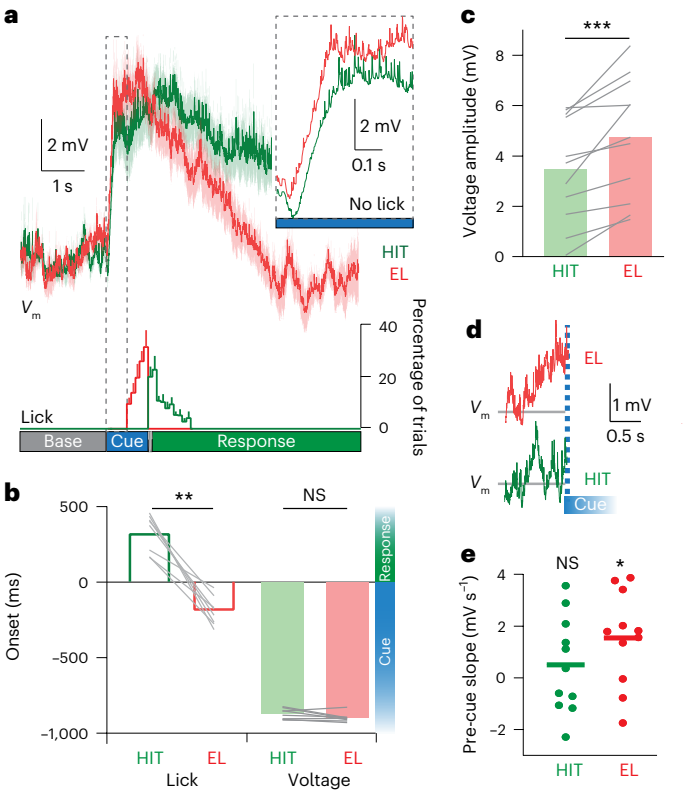

Fig. 6 | The cue-evoked voltage response during premature behavior is larger than during correct behavior. a, Overlaid grand averages (dark color trace) and standard error (light color trace) of the voltage response during EL (red) and HIT (green) trials in the cued sensory association task. Insert, magnification of voltage during the auditory cue when there was no licking behavior. **b**, Onset of the licking (left) and voltage (right) response during HIT (green) and EL (red) trials (licking, $P = 0.008$, two-tailed Wilcoxon test; voltage, $P = 0.11$, two-tailed Wilcoxon test; $n = 8$ neurons, 4 mice). **c**, Amplitude of the voltage response in HIT and EL trials ($P = 0.001$, two-tailed Wilcoxon test; $n = 11$ neurons, 4 mice). **d**, Grand average membrane potential during HIT (green) and EL (red) trials 1 s before the auditory cue onset. **e**, The slope of the membrane potential before the auditory cue in HIT (green) and EL (red) trials (HIT, $P = 0.46$, two-tailed one-sample Wilcoxon test; EL, $P = 0.02$, two-tailed one-sample Wilcoxon test; $n = 11$ neurons, 4 mice). NS, $P > 0.05$; $^{*}P < 0.05$; $^{**}P < 0.01$; $^{***}P < 0.001$.

be due partially to long-term plasticity as sequences of sensory events in the environment can be quickly engraved in cortical circuitry[28–30]. However, plasticity cannot fully explain the findings reported in this study because the voltage responses were heavily dependent on task engagement and performance. This is clearly illustrated by comparing the HIT and MISS trials, which evoked different voltage responses to the same auditory cue. Furthermore, as previously reported in primary cortices[31,32], arousal could be a substantial component adding to the voltage response during the cue. However, our findings suggest that ALM neurons encode anticipatory behavior beyond arousal as, despite similar levels of cue-evoked arousal during HIT and MISS trials, the voltage responses were substantially different. To further explore the relationship between the ALM and arousal, dedicated experiments where pupil dilation and ALM activity are measured simultaneously are needed.

In this study, an auditory cue preceded a tactile stimulus which informed the animal about the upcoming response window and possible reward. Mice may use a number of strategies to perform this task, including relying on the occurrence of the tactile stimulus and/or the timing of the instructive cue. Here, mice appeared to use both strategies, since (1) changing the duration of the cue influenced the rate and the timing of the EL responses and (2) omission of either the auditory cue or tactile stimulus decreased performance in the task. Similar to previous studies[11,13], the introduction of a cue led to the emergence of EL responses. The strong influence of the cue on impulsive behavior is highlighted in this study as mice aborted approximately 40% of the Go trials, which was consistent throughout training. During this premature impulsive behavior, suppressing ALM activity during the auditory cue, but not reward period, decreased the rate and increased the latency of the premature licking. Although the influence of ALM suppression on the response latency was relatively small, similar delays of movement in trained motor actions were previously reported during disruption of cortical preparatory activity in both primates[33] and mice[5]. ALM suppression during the auditory cue also decreased the reaction time, but not overall rate, during correct performance. Combined, the voltage recordings and photo-inhibition results are complimentary, as inhibiting the ALM during the behavior with the largest voltage response (EL) had the greatest influence on behavioral performance. It is, however, puzzling as to why suppressing ALM during the auditory cue led to decreased reaction times during correct performance. This is not due to rebound following ALM suppression since the firing rate of ALM neurons returned to baseline following photo-inhibition, and may instead be due to an overall shift in the timing of EL distributions.

https://doi.org/10.1038/s41593-022-01198-z

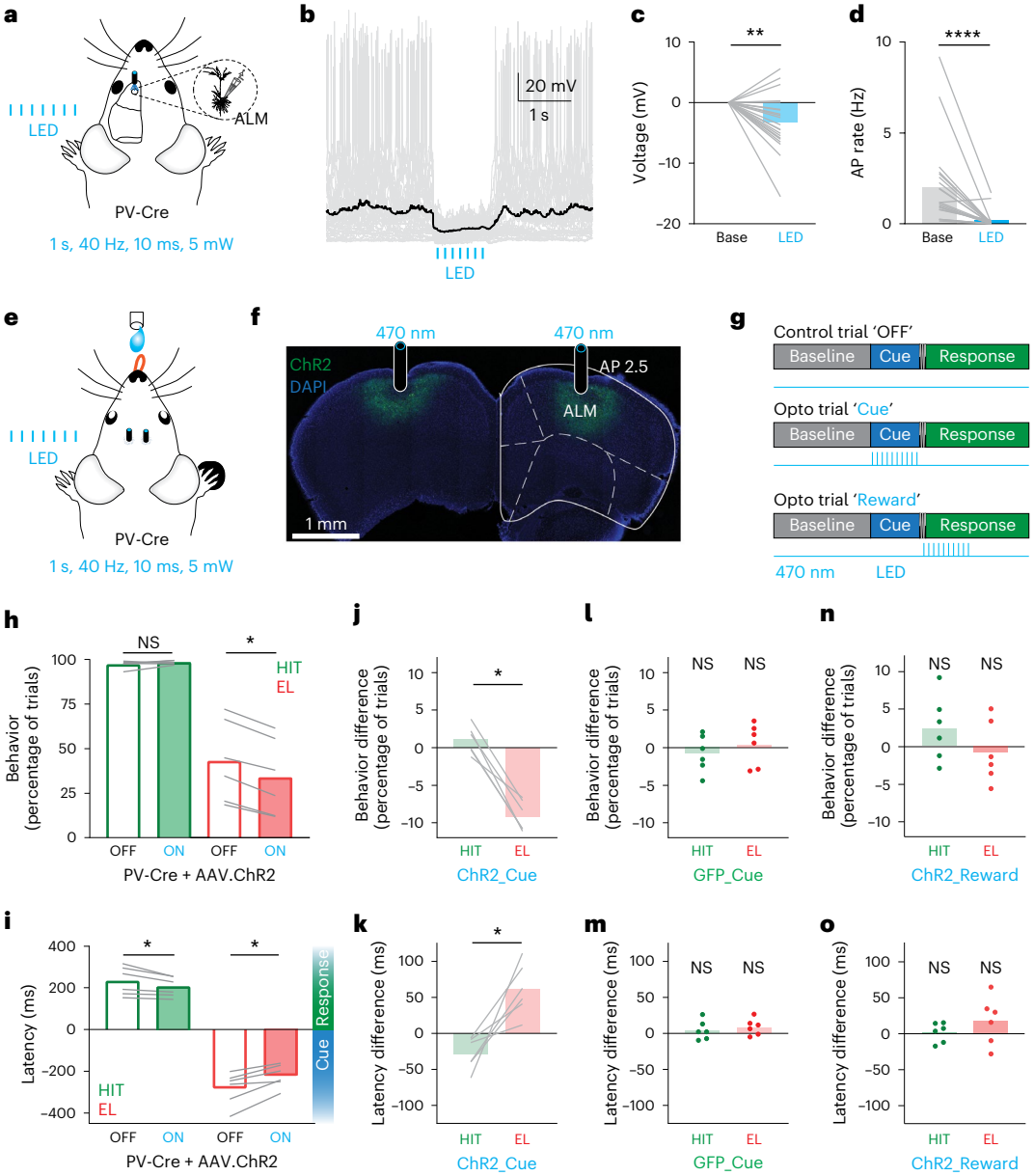

Fig. 7 | Suppression of ALM activity during the auditory cue reduces impulsive premature behavior. a, Experimental design. Whole-cell patch-clamp recordings were performed from pyramidal neurons within the ALM (AP 2.5, ML 1.5 from bregma) in anesthetized PV$^+$ Cre mice previously injected with light-sensitive opsin ChR2 (pAAV-EF1a-doublefloxed-hChR2(H134R)-EYFP-WPRE-HGHpA) into the ALM. Blue LED pulses (470 nm, 40 Hz, 10 ms, 2–5 mW) were used to activate ChR2. **b**, Overlay of voltage traces from an L2/3 pyramidal neuron within ALM during photo-activation of PV interneurons. **c**, Voltage response in ALM L2/3 pyramidal neurons during photo-activation of PV interneurons, normalized to baseline membrane potential ($P = 0.004$, two-tailed Wilcoxon test; $n = 21$ neurons, 5 mice). **d**, Firing rate of ALM pyramidal neurons during photo-activation of PV interneurons ($P < 0.0001$, two-tailed Wilcoxon test; $n = 21$ neurons, 5 mice). **e**, Experimental design. During the cued sensory association task, the ALM was suppressed by blue LED pulses (470 nm, 40 Hz, 10 ms, 2–5 mW) delivered to PV$^+$ Cre mice bilaterally injected with light-sensitive opsin ChR2 into the ALM. **f**, Example confocal image of a brain slice from a PV$^+$ Cre mouse bilaterally injected with ChR2 into the ALM (AP 2.5, ML 1.5). Post hoc injection and virus expression verification were done with all injected animals ($n = 12$ mice). **g**, During the cued sensory association task, blue LED pulses (470 nm, 40 Hz, 10 ms, 5 mW) were delivered during the auditory cue (top, Opto trial 'Cue') or reward window (bottom, Opto trial 'Reward') in 50% of randomly interleaved Go trials. No LED pulses were delivered during the Control trial 'OFF' (50% of trials). **h**, The rates of HIT and EL trials during LED ON and OFF during the auditory cue in PV$^+$ Cre mice previously injected with ChR2 into ALM (HIT, $P = 0.44$, two-tailed Wilcoxon test; EL, $P = 0.03$, two-tailed Wilcoxon test; $n = 6$ mice). **i**, The average latency of the first lick response in HIT and EL trials during LED ON and OFF during the auditory cue in PV$^+$ Cre mice previously injected with ChR2 into ALM (HIT, $P = 0.03$, two-tailed Wilcoxon test; EL, $P = 0.03$, two-tailed Wilcoxon test; $n = 6$ mice). **j**, Photo-inhibition of ALM during the cue significantly influenced the rate of EL trials compared with HIT trials in PV$^+$ Cre mice previously injected with ChR2 into ALM ($P = 0.03$, two-tailed Wilcoxon test; $n = 6$ mice). **k**, Photo-inhibition of ALM during the cue had a greater influence on the latency to the first lick response during EL trials compared with HIT trials ($P = 0.03$, two-tailed Wilcoxon test; $n = 6$ mice). **l**, The rate change in HIT and EL trials during photo-inactivation throughout the auditory cue in control PV$^+$ Cre mice previously injected with muGFP into ALM (HIT, $P = 0.44$, two-tailed Wilcoxon test; EL, $P = 0.84$, two-tailed Wilcoxon test; $n = 6$ mice). **m**, The effect on the lick latency in HIT and EL trials during photo-inactivation during the cue in control PV$^+$ Cre mice previously injected with muGFP into ALM (HIT, $P = 0.56$, two-tailed Wilcoxon test; EL, $P = 0.22$, two-tailed Wilcoxon test; $n = 6$ mice). **n**, The rate change of HIT and EL trials during photo-inactivation during the reward window in PV$^+$ Cre mice previously injected with ChR2 into ALM (HIT, $P = 0.31$, two-tailed Wilcoxon test; EL, $P = 0.69$, two-tailed Wilcoxon test; $n = 6$ mice). **o**, The effect on the lick latency in HIT and EL trials during photo-inactivation in the reward window in PV$^+$ Cre mice previously injected with ChR2 into ALM (HIT, $P = 0.99$, two-tailed Wilcoxon test; EL, $P = 0.31$, two-tailed Wilcoxon test; $n = 6$ mice). NS, $P > 0.05$; *$P < 0.05$; **$P < 0.01$; ****$P < 0.0001$.

Although the cause is unknown, the effect of ALM photo-inhibition on licking behavior during correct performance was significantly less than during premature behavior, highlighting the greater influence of ALM activity during premature action. In contrast to our findings, previous studies have shown that inhibition of ALM leads to almost complete abolishment of licking[34]. This discrepancy in results may be explained by the different inhibitory methods and/or behavioral tasks used[2–5,10].

In addition to a large cue-evoked voltage response, our findings also illustrate that premature behavior was characterized by a gradual ramping depolarization of ALM neurons before the onset of the auditory cue. Ramping of neural activity in anticipation of movement has also been previously recorded in the ALM of nonhuman primates[35,36]. This ramping depolarization may contribute to the larger cue-evoked voltage responses reported in EL trials and may be a result of a time-fixed behavioral protocol[4]. However, despite the same auditory cue, ramping depolarization only occurred during premature, and not correct, behavior. What is the potential microcircuit underlying the voltage ramp and cue-evoked voltage response in ALM neurons? Due to the increased dopamine signaling during sensory cues and reward delivery[37,38], and the direct connectivity between the reward pathway and prefrontal cortex (PFC)[39,40], direct input from the basal ganglia is a prime candidate for driving impulsive activity in the ALM[11,41,42]. Alternatively, the basal ganglia may indirectly drive the ALM through the ventromedial thalamus, which influences the speed of behavioral responses[43] and plays a role in impulsive actions[18]. Interestingly, the influence of ALM on premature impulsive behavior is in contrast to the PFC, which has been shown to curb impulsive behavior[15,19,42]. Overall, it is evident that the control of impulsive premature behavior involves multiple brain regions (PFC, basal ganglia, thalamus and ALM) and further unraveling the pathway driving impulsive behavior is an exciting direction for future research.

Motor behavior is widely encoded throughout the cortex[44,45]. ALM activity recorded during the cued sensory association task could, at least in part, be attributed to motor output, especially the long-lasting response during correct HIT trials where the animal licks to retrieve the water reward. However, in our study, the task was designed to discourage mice from licking during the cue presentation to avoid the contribution of motor activity during the cue presentation. Typically, it takes less than 200 ms from the onset of the lick movement for the tongue reach a water spout[26]. Therefore, in our study we only analyzed the voltage response at the beginning of the cue, and well before licking behavior, to avoid the possible contribution from licking-associated movements. Although other types of motor activity, such as unspecific orofacial movements, could be also present before the lick is initiated, our recordings of EMG activity from nuchal musculature did not detect a substantial motor response at the onset of the cue. Combined with previous findings using high-speed videography that did not show any substantial orofacial movements before licking onset[18], our findings suggest that the voltage response recorded at the onset of the cue is not motor induced. Furthermore, M1 neurons only had a small ramping voltage throughout the auditory cue, suggesting that the large cue-evoked response in ALM neurons is not due to generalized motor activity. Lastly, despite the timing difference in licking behavior, the onset of the voltage responses during both the HIT and EL trials was similar, suggesting that the voltage onset in ALM neurons is not simply motor activity dependent.

Taken together, these data expand the known roles of the ALM. Previous studies have illustrated that the ALM is involved in the motor planning of skilled movements[2–4,23]. Here, we illustrate that L2/3 pyramidal neurons within the ALM also encode and influence premature impulsive behavior. Since L2/3 pyramidal neurons control the gain of layer 5 pyramidal neurons[46], preparatory activity in L2/3 pyramidal neurons within the ALM would have both a local and lateral cortical influence. These results highlight the fragility of the microcircuitry driving cued behavior, where relatively small changes in cellular voltage can be correlated with large changes in behavioral outcome.

Online content

Any methods, additional references, Nature Research reporting summaries, source data, extended data, supplementary information, acknowledgements, peer review information; details of author contributions and competing interests; and statements of data and code availability are available at https://doi.org/10.1038/s41593-022-01198-z.

References

1. Bruce, C. J. & Goldberg, M. E. Primate frontal eye fields. I. Single neurons discharging before saccades. *J. Neurophysiol.* **53**, 603–635 (1985).
2. Chen, T. W., Li, N., Daie, K. & Svoboda, K. A map of anticipatory activity in mouse motor cortex. *Neuron* **94**, 866–879 e4 (2017).
3. Guo, Z. V. et al. Flow of cortical activity underlying a tactile decision in mice. *Neuron* **81**, 179–194 (2014).
4. Inagaki, H. K., Fontolan, L., Romani, S. & Svoboda, K. Discrete attractor dynamics underlies persistent activity in the frontal cortex. *Nature* **566**, 212–217 (2019).
5. Li, N., Guo, Z. V., Chen, T. W. & Svoboda, K. in *Micro-, Meso- and Macro-Dynamics of the Brain* (eds Buzsaki, G. & Christen, Y.) (Springer, Cham (CH), 2016).
6. Gao, Z. et al. A cortico-cerebellar loop for motor planning. *Nature* **563**, 113–116 (2018).
7. Gilad, A., Gallero-Salas, Y., Groos, D. & Helmchen, F. Behavioral strategy determines frontal or posterior location of short-term memory in neocortex. *Neuron* **99**, 814–828.e7 (2018).
8. Maimon, G. & Assad, J. A. A cognitive signal for the proactive timing of action in macaque LIP. *Nat. Neurosci.* **9**, 948–955 (2006).
9. Nobre, A. C. & van Ede, F. Anticipated moments: temporal structure in attention. *Nat. Rev. Neurosci.* **19**, 34–48 (2018).
10. Svoboda, K. & Li, N. Neural mechanisms of movement planning: motor cortex and beyond. *Curr. Opin. Neurobiol.* **49**, 33–41 (2018).
11. Coddington, L. T. & Dudman, J. T. The timing of action determines reward prediction signals in identified midbrain dopamine neurons. *Nat. Neurosci.* **21**, 1563–1573 (2018).
12. Dalley, J. W., Everitt, B. J. & Robbins, T. W. Impulsivity, compulsivity, and top-down cognitive control. *Neuron* **69**, 680–694 (2011).
13. Lee, K. et al. Temporally restricted dopaminergic control of reward-conditioned movements. *Nat. Neurosci.* **23**, 209–216 (2020).
14. Otis, J. M. et al. Prefrontal cortex output circuits guide reward seeking through divergent cue encoding. *Nature* **543**, 103–107 (2017).
15. Kim, S. & Lee, D. Prefrontal cortex and impulsive decision making. *Biol. Psychiatry* **69**, 1140–1146 (2011).
16. Dalley, J. W. & Ersche, K. D. Neural circuitry and mechanisms of waiting impulsivity: relevance to addiction. *Philos. Trans. R. Soc. Lond. B Biol. Sci.* **374**, 20180145 (2019).
17. Dalley, J. W. & Roiser, J. P. Dopamine, serotonin and impulsivity. *Neuroscience* **215**, 42–58 (2012).
18. Catanese, J. & Jaeger, D. Premotor ramping of thalamic neuronal activity is modulated by nigral inputs and contributes to control the timing of action release. *J. Neurosci.* **41**, 1878–1891 (2021).
19. Li, B., Nguyen, T. P., Ma, C. & Dan, Y. Inhibition of impulsive action by projection-defined prefrontal pyramidal neurons. *Proc. Natl Acad. Sci. USA* **117**, 17278–17287 (2020).
20. Ebbesen, C. L. et al. More than just a 'motor': recent surprises from the frontal cortex. *J. Neurosci.* **38**, 9402–9413 (2018).
21. Miri, A. et al. Behaviorally selective engagement of short-latency effector pathways by motor cortex. *Neuron* **95**, 683–696 e11 (2017).
22. Galinanes, G. L., Bonardi, C. & Huber, D. Directional reaching for water as a cortex-dependent behavioral framework for mice. *Cell Rep.* **22**, 2767–2783 (2018).

23. Li, N., Chen, T. W., Guo, Z. V., Gerfen, C. R. & Svoboda, K. A motor cortex circuit for motor planning and movement. *Nature* **519**, 51–56 (2015).
24. Bradley, M. M., Miccoli, L., Escrig, M. A. & Lang, P. J. The pupil as a measure of emotional arousal and autonomic activation. *Psychophysiology* **45**, 602–607 (2008).
25. Reimer, J. et al. Pupil fluctuations track fast switching of cortical states during quiet wakefulness. *Neuron* **84**, 355–362 (2014).
26. Bollu, T. et al. Cortex-dependent corrections as the tongue reaches for and misses targets. *Nature* **594**, 82–87 (2021).
27. Banerjee, A. & Long, M. A. Ready, steady, go! Imaging cortical activity during movement planning and execution. *Neuron* **94**, 698–700 (2017).
28. Fiser, A. et al. Experience-dependent spatial expectations in mouse visual cortex. *Nat. Neurosci.* **19**, 1658–1664 (2016).
29. Gavornik, J. P. & Bear, M. F. Learned spatiotemporal sequence recognition and prediction in primary visual cortex. *Nat. Neurosci.* **17**, 732–737 (2014).
30. Jaramillo, S. & Zador, A. M. The auditory cortex mediates the perceptual effects of acoustic temporal expectation. *Nat. Neurosci.* **14**, 246–251 (2011).
31. Lin, P.-A., Asinof, S. K., Edwards, N. J. & Isaacson, J. S. Arousal regulates frequency tuning in primary auditory cortex. *Proc. Natl Acad. Sci. USA* **116**, 25304–25310 (2019).
32. McGinley, M. J., David, S. V. & McCormick, D. A. Cortical membrane potential signature of optimal states for sensory signal detection. *Neuron* **87**, 179–192 (2015).
33. Churchland, M. M., Yu, B. M., Ryu, S. I., Santhanam, G. & Shenoy, K. V. Neural variability in premotor cortex provides a signature of motor preparation. *J. Neurosci.* **26**, 3697–3712 (2006).
34. Komiyama, T. et al. Learning-related fine-scale specificity imaged in motor cortex circuits of behaving mice. *Nature* **464**, 1182–1186 (2010).
35. Funahashi, S., Bruce, C. J. & Goldman-Rakic, P. S. Mnemonic coding of visual space in the monkey's dorsolateral prefrontal cortex. *J. Neurophysiol.* **61**, 331–349 (1989).
36. Riehle, A. & Requin, J. Monkey primary motor and premotor cortex: single-cell activity related to prior information about direction and extent of an intended movement. *J. Neurophysiol.* **61**, 534–549 (1989).
37. Schultz, W., Apicella, P. & Ljungberg, T. Responses of monkey dopamine neurons to reward and conditioned stimuli during successive steps of learning a delayed response task. *J. Neurosci.* **13**, 900–913 (1993).
38. Mirenowicz, J. & Schultz, W. Preferential activation of midbrain dopamine neurons by appetitive rather than aversive stimuli. *Nature* **379**, 449–451 (1996).
39. Mininni, C. J., Caiafa, C. F., Zanutto, B. S., Tseng, K. Y. & Lew, S. E. Putative dopamine neurons in the ventral tegmental area enhance information coding in the prefrontal cortex. *Sci. Rep.* **8**, 11740 (2018).
40. Perez-Lopez, J. L., Contreras-Lopez, R., Ramirez-Jarquin, J. O. & Tecuapetla, F. Direct glutamatergic signaling from midbrain dopaminergic neurons onto pyramidal prefrontal cortex neurons. *Front. Neural Circuits* **12**, 70 (2018).
41. Schultz, W., Dayan, P. & Montague, P. R. A neural substrate of prediction and reward. *Science* **275**, 1593–1599 (1997).
42. Miller, E. K. The prefrontal cortex and cognitive control. *Nat. Rev. Neurosci.* **1**, 59–65 (2000).
43. Takahashi, N. et al. Thalamic input to motor cortex facilitates goal-directed action initiation. *Curr. Biol.* **31**, 4148–4155 e4 (2021).
44. Stringer, C. et al. Spontaneous behaviors drive multidimensional, brainwide activity. *Science* **364**, 255 (2019).
45. Musall, S., Kaufman, M. T., Juavinett, A. L., Gluf, S. & Churchland, A. K. Single-trial neural dynamics are dominated by richly varied movements. *Nat. Neurosci.* **22**, 1677–1686 (2019).
46. Quiquempoix, M. et al. Layer 2/3 pyramidal neurons control the gain of cortical output. *Cell Rep.* **24**, 2799–2807 e4 (2018).

Methods

All procedures were approved by the Florey Institute of Neuroscience and Mental Health Animal Care and Ethics Committee (18-035-FINHMH) and followed the guidelines of the Australian Code of Practice for the Care and Use of Animals for Scientific Purposes.

Mice

Wild-type C57BL/6 (postnatal 28–60; Australian Resource Centre) and PV^{+} Cre (postnatal 28–60; The Jackson Laboratory no. 008069) female mice were used in this study. Mice were housed in groups of up to six individuals in a 12:12 natural light/dark cycle. Room temperature was kept constant at 18–24 °C and humidity at 40–70%. All experiments were performed during the light phase.

Head-post implantation for stabilization

To surgically implant the head-post onto the skull for head stabilization, mice were anesthetized with isoflurane (1–2% in 0.75 l min^{-1} O_2). Body temperature was maintained at 36 °C and the depth of anesthesia was monitored throughout the surgery. Eye ointment was applied to prevent dehydration and the top of the head was disinfected with 70% ethanol and betadine. Lidocaine (20 mg ml^{-1}, Ilium) was topically injected around the surgical site before the skin was cut to expose the skull. A custom-made metal head-post (2 × 1 × 0.1 cm^3) was then attached to the skull using dental cement (C&B Metabond, Parkell). A subset of mice were implanted with Teflon-coated stainless-steal electrodes into nuchal muscles bilaterally to record gross motor activity. Meloxicam (3 mg kg^{-1}) was injected intraperitoneally (i.p.) for additional postoperative analgesia and anti-inflammatory action. Mice were then returned to their cages to recover (~1 week).

Habituation and behavioral training

Mice with implanted head-posts were gradually habituated to head restriction over 2–4 d. During this period, mice were handled and acclimatized to the behavioral setup. First, mice were head restrained for incremental periods of time (5 s to 2 min) until habituated to head restraint. Then, mice were head-fixed to the recording frame for 2–4 sessions of up to 15 min each, where mice rested their forepaws unaided on either an inactive (ipsilateral) or active (contralateral) piezo-electric buzzer driven by an Arduino Uno microprocessor. Once habituated to the experimental setup, behavioral training commenced. To maximize task engagement, 1 d before the beginning and throughout behavioral training, mice were water restricted (1 ml d^{-1} of 10% sucrose water). Behavioral training was performed in three main phases using a Bpod behavioral platform (Bpod State Machine r1, Sanworks). Phase 1: mice were trained to associate tactile stimulation with sucrose reward delivery (10 µl; 10% sucrose in water) by licking a water spout. Sucrose water delivery was paired with tactile stimulation of the contralateral forepaw (0.1 s; 200 Hz). Phase 2: mice were trained to lick in response to tactile stimulation. Licking was detected using an optical lickometer (Sanworks). Here, sucrose water reward was only delivered if the mouse licked the water spout within 1 s after the tactile stimulus was delivered. Only correct responses (licks during response epoch) were rewarded (HIT) while failure to report the stimulus was considered as an incorrect response (MISS) and no reward was delivered. Trials with no tactile stimulation (Catch trials) were randomly interleaved with Go trials. Trials had randomized 2–4-s intertrial interval with 0.7/0.3 Go/Catch trial ratio, respectively. Licking during Catch trials was considered as a false alarm while withhold the licking as correct rejection. Mice were not rewarded during correct rejection and no punishment was used for false alarm. Furthermore, no licking was allowed during the 2-s baseline period before the onset of the stimulus. If mice licked within the baseline period, the trial was aborted. Once the mice reached d′ > 1, they were transferred into phase 3. Phase 3: an auditory cue (1 s; 7 kHz; 60 dB) was delivered before the tactile stimulus. To receive a sucrose water reward, the mouse had to withhold licking during the auditory cue and lick the water port only during or within 1 s after the tactile stimulation was delivered (0.1 s; 200 Hz; HIT). If mice did not lick the water port during the response epoch, the trial was classified as MISS. If licking occurred during the auditory cue, the trial was aborted (EL) and no reward was delivered. Interleaved trials with no sensory stimulation (Catch trials) were used to evaluate spontaneous licking. Mice were trained in phase 3 for at least 3 consecutive days and had to reach d′ > 1. HIT and false alarm rates were calculated as follows: $\text{HIT\_rate} = \left(\frac{\text{HIT trials}}{\text{(all trials−EL trials)}}\right) \times 100\%$; FA_rate = 1 − HIT_rate.

Both the behavioral performance (HIT and false alarm rates) and speed of the behavioral response were analyzed. Here, the latency to the first lick was considered for both HIT and EL trials and aligned to the onset of the tactile stimulation. Either distribution of the latencies (Fig. 1d,g,h) or mean latencies (Fig. 1e,f) were quantified.

In total, 32 mice were trained in the cued sensory association task. Different recordings (whole-cell patch-clamp, pupil tracking) or manipulation (optogenetic inactivation) were performed on a subset of these mice. Naïve mice, after initial habituation to head restraint, were presented with an auditory stimulus (1 s; 7 kHz; 60 dB) immediately followed by a tactile stimulus (0.1 s; 200 Hz) for multiple sessions over 4–6 d.

Whole-cell patch-clamp recordings

Mice (C57BL/6), which had previously had a head-post implanted (>5 d earlier) and underwent a habituation and/or training phase, were anesthetized with isoflurane (1–2% in 0.75 l min^{-1} O_2) and a craniotomy (1 × 1 mm^2) was performed over the ALM (anteroposterior (AP), 2.5 mm; mediolateral (ML), 1.5 mm) and M1 (AP 0.25 mm, ML 1.5 mm). Recordings from M1 neurons were performed from either the same mice where recordings were also performed in ALM (2 of 6 mice) or separate mice (4 of 6 mice). The duration of the training and rate of EL trials were similar for mice where recordings were performed in M1 (4.83 ± 0.4 d of training, 31.85 ± 5.19% EL rate, n = 6 mice) and ALM (5.5 ± 0.87 d of training, 32.5 ± 3.66% EL rate, n = 4 mice). The brain was covered with agar and inert silicon (kwik-cast, WPI). Meloxicam (3 mg kg^{-1}) was injected i.p. for additional postoperative analgesia and anti-inflammatory action. Mice were allowed to recover for at least 2 h in their home cage before whole-cell patch-clamp recordings were performed. During a recording session, mice were head-fixed and the silicon protective cover was removed, and ringer (135 mM NaCl, 5.4 mM KCl, 1.8 mM $CaCl_2$, 1 mM $MgCl_2$, 5 mM HEPES) was used to bathe the craniotomy throughout the experiment. Whole-cell recordings were obtained from L2/3 pyramidal neurons (~200 µm below pia) using a patch pipette (resistance 4–6 MΩ) filled with an intracellular solution containing 115 mM potassium gluconate, 20 mM KCl, 10 mM sodium phosphocreatine, 10 mM HEPES, 4 mM Mg-ATP, 0.3 mM Na-GTP, adjusted to pH 7.3–7.4 with KOH. The patch pipette was inserted into the brain at an angle of 45° or 80° relative to the cortical surface, to a depth of ~100 µm, and then advanced in steps of 2 µm until a neuron was encountered. The average depth of recorded neurons was 241 ± 12 µm (n = 36 neurons, 8 mice). Recordings were made in current-clamp configuration using a Dagan BVC-700A amplifier and sampled at 20 kHz with no bias current injected unless otherwise stated. Successfully patched neurons typically had low (<50 MΩ) access resistance upon break-in. The average number of recorded trials was 37.31 ± 2.96 and the average resting membrane potential was −58.01 ± 1.11 mV with no junction potential correction (n = 36 neurons, 8 mice). In experiments where the influence of photo-activation of PV interneurons on the firing rate of pyramidal neurons was assessed, positive current (73.81 ± 16.04 pA on average, n = 21 neurons) was injected to facilitate action potential generation. Custom-written Igor Pro (v.6.3, Wavemetrics) software was used for both acquisition and analysis. The identity of the recorded pyramidal cell in in vivo blind recordings was confirmed using the recording depth and voltage response to current steps. Voltage recordings were performed in either expert mice as they performed the task or naïve

mice that were passively exposed to the auditory and tactile stimulation protocol.

Nuchal EMG recordings and analysis

EMG activity was recorded using a differential amplifier (DB-301, Warner Instruments) using 20-kHz sampling. The EMG signal was filtered from 300 Hz to 10 kHz, rectified and down-sampled to 1 kHz. The EMG was sorted according to trial outcome, averaged and normalized to its maximal activity.

Analysis of whole-cell patch-clamp recordings

L2/3 pyramidal neurons from ALM (n = 16 neurons, 4 mice) and M1 (n = 20 neurons, 6 mice) were recorded during the cued sensory association task. Due to sensitivity to movement, whole-cell recordings typically do not last long. Here, 36.76 ± 2.93 trials of 8-s episodes were recorded on average. Recorded voltage responses of pyramidal neurons were grouped according to the trial outcome, that is, HIT, EL and MISS. Only neurons with >3 trials for a particular trial outcome were further analyzed during that trial outcome. Due to short-lasting whole-cell recording, some neurons had only certain but not all trial types, and therefore when paired statistics is being used, the number of neurons reported in the Results section appears lower. Furthermore, analysis was aborted if action potential amplitude abruptly decreased by greater than 30% or if the resting voltage deviated rapidly and substantialy from baseline. To quantify voltage response to auditory cue, membrane potentials recorded during multiple trials were averaged and baseline (2 s before stimulation) subtracted. Action potential rate was calculated for each 100-ms time bin for each neuron. Because of sparse coding of L2/3 neurons, some neurons generate very few action potentials throughout short whole-cell recordings. Only neurons with >5 action potentials were used for analysis, which results in lower number of neurons reported in the Results section. The onset of voltage response was detected from averaged voltage traces by using the threshold, which was baseline membrane potential + 2 s.d. of baseline membrane potential. Neurons without measurable voltage response (baseline + 2 s.d.) were not included in the analysis which results in lower numbers of neurons reported in the Results.

Optogenetic inactivation of frontal cortex

PV^+ Cre mice were anesthetized with isoflurane (1–2% in 0.75 l min^{-1} O_2) and placed in a stereotaxic frame (Narishige). Body temperature was maintained at 36 °C and the depth of anesthesia was monitored throughout the surgery. Eye ointment was applied to prevent dehydration and the top of the head was disinfected with 70% ethanol and betadine. Lidocaine (20 mg ml^{-1}, Ilium) was topically injected around the surgical site before the skin was cut to expose the skull. Small craniotomies (0.5 × 0.5 mm^2) were made over ALM bilaterally using the following stereotaxic coordinates: anteroposterior (AP), 2.5 mm; mediolateral (ML), 1.5 mm. AAV1 virus (100 nl, pAAV-EF1a-doublefloxed-hChR2(H134R)-EYFP-WPRE-HGHpA or AAV1/2-muGFP (ref. [47])) was slowly injected from a glass pipette (Wiretrol, Drummond) inserted 0.3 mm deep in the cortex for at least 5 min using an oil hydraulic manipulator system (MMO-220A, Narishige). Following virus injection, a custom-made fiber optic cannula (FT400EMT, 400 µm 0.39 NA, 1-mm fiber, Thorlabs) was slowly lowered down the injection track using a stereotaxic arm until the desired depth was reached (0.1 mm from pia). Dental cement (C&B Metabond, Parkell) was then applied around the edges of the cannula to secure it to the skull and left to dry for ~5 min. The same dental cement was used to attach a custom-made aluminum head-post (2 × 1 × 0.1 cm^3) to the skull for head-fixation. Meloxicam (3 mg kg^{-1}) was injected i.p. for additional postoperative analgesia and anti-inflammatory action. Mice were then returned to their cages to recover for ~1 week before behavioral training in the cued sensory association task commenced (Habituation and behavioral training). Mice performed the cued sensory association task for several days before optogenetic experimental sessions were performed (3–6 sessions over 3 consecutive days). Photo-inactivation of the ALM was achieved by delivering a train of light pulses (470 nm, 10 ms, 40 Hz for 1 s, 5 mW) through an optical fiber (FT400EMT, Thorlabs) directly attached to the cannula (FT400EMT, 400 µm 0.39 NA, 1-mm fiber, Thorlabs). An LED driver (LEDD1B, Thorlabs) coupled to a 470-nm LED (M470F3, Thorlabs) was used to generate the train of light pulses. The train of light pulses was initiated at the same time as the auditory cue and lasted throughout the cue. A custom-made shield was placed over optic fibers and cannulas to prevent scattered light from entering the animal's visual field. An additional background of blue light (delivered through LED; M470L4-C1, Thorlabs) was used above the mouse's head during the training sessions and the optogenetic silencing experiment. Trials with the train of light pulses (LED ON) and without (LED OFF) were randomly interleaved at a rate of 50% each. Custom routines in MATLAB were used to operate the behavioral platform and data acquisition.

Pupil tracking and analysis

To monitor engagement during sensory-based behavior, pupil tracking was performed in a subset of mice previously trained in the cued sensory association task (n = 10 mice) or naïve mice exposed to the auditory and tactile stimulation (n = 11 mice). Mice were head-fixed and the left eye illuminated with infrared light (850-nm LED, Thorlabs). This illumination did not affect pupil diameter. An infrared-sensitive high-speed CMOS camera (Basler acA1300-200um) mounting a 50-mm lens (Kowa 50 mm/F2.8) was used to image pupil dynamics at 15 frames per second. Frames were triggered externally using an Arduino microprocessor connected to a Bpod. Changes in pupil diameter were recorded and measured online using a custom software (Pylon-PD, Eridian Systems, Berlin, Germany) kindly provided by Viktor Bahr, Jens Kremkow and Robert Sachdev and colleagues[48]. Pupil dilation was calculated as a percentage change and normalized to the baseline pupil diameter (1 s before the auditory cue). Pupil dilation during the auditory cue was evaluated as mean pupil diameter 0.5 s after the auditory cue onset (0.5-s time window). Pupil dilation during the reward window was evaluated as mean pupil diameter 0.5 s after the auditory cue termination (1.5-s time window). Only sessions where pupil was measured during >5 of the same trial types (for example, HIT or MISS) were used for analysis.

Data analysis

Custom-written Igor Pro software (v.6.3, WaveMetrics) was used for the acquisition and analysis of whole-cell electrical recordings. Behavior was analyzed using custom-written MATLAB 2019a codes.

Statistics and reproducibility

Statistics were performed using Prism software (v.9, GraphPad). Normality tests were performed and significance was determined using two-sided nonparametric tests (one-sample Wilcoxon test; Wilcoxon matched-pairs signed rank test for paired comparison; Mann–Whitney test for unpaired comparison) at a significance level of 0.05 and no adjustments were made for multiple comparisons. Specific statistical tests used and sample sizes are indicated in figure captions and text. No statistical method was used to predetermine sample size but our sample sizes are similar to those reported in previous publications[32,43]. No data were excluded from the analyses and experiments were not randomized as all mice were trained and recorded under the same conditions. Every finding in the manuscript was shown in multiple mice and therefore replicated across mice. Since the analysis procedures were either fully or semiautomated, the investigators were not blinded to allocation during experiments and outcome assessment. Unless otherwise stated, the data are presented as mean ± s.e.m.

Reporting summary

Further information on research design is available in the Nature Portfolio Reporting Summary linked to this article.

Data availability

Data supporting the findings of this study are available within the paper and its Supplementary Information files. Source data are provided with this paper.

Code availability

Source code for acquisition and analysis of voltage recordings is available by request.

References

47. Scott, D. J. et al. A novel ultra-stable, monomeric green fluorescent protein for direct volumetric imaging of whole organs using CLARITY. *Sci. Rep.* **8**, 667 (2018).
48. Bergmann, R. et al. Coordination between eye movement and whisking in head-fixed mice navigating a plus maze. *eNeuro* https://doi.org/ENEURO.0089-22.2022 (2022).

Acknowledgements

We thank D. Scott for providing the AAV1/2-muGFP and V. Bahr, J. Kremkow and R. Sachdev for custom software for measuring online pupil diameter. This work was supported by the NHMRC (grant nos. APP1086082 and APP1063533, L.M.P.), the Sylvia and Charles Viertel Charitable Foundation (L.M.P.), the Australian Research Council (grant no. DP160103047, L.M.P.), IBRO (Return Home Fellowship and Early Career Award, R.G.) and an MJJ (Marius Jakulis Jason) fellowship (R.G.). The funders had no role in study design, data collection and analysis, decision to publish or preparation of the manuscript.

Author contributions

R.G. and L.M.P. conceptualized and designed the study. R.G. performed and analyzed all experiments. L.G. performed control opto-inactivation experiments. R.G. and L.M.P. interpreted the results and wrote the paper.

Competing interests

The authors declare no competing interests.

Additional information

Extended data is available for this paper at https://doi.org/10.1038/s41593-022-01198-z.

Supplementary information The online version contains supplementary material available at https://doi.org/10.1038/s41593-022-01198-z.

Correspondence and requests for materials should be addressed to Robertas Guzulaitis or Lucy Maree Palmer.

Peer review information *Nature Neuroscience* thanks the anonymous reviewers for their contribution to the peer review of this work.

https://doi.org/10.1038/s41593-022-01198-z

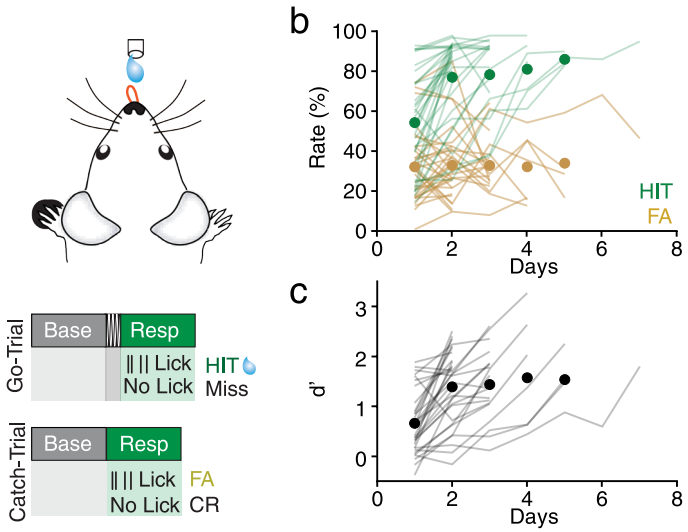

Extended Data Fig. 1 | Performance in tactile association task. (**a**) The tactile-association task design. Mice were trained to lick a water port within 1 s of a tactile stimulation delivered to the forepaw (200 Hz, 100 ms). Correct responses (HIT) were rewarded with sucrose water (5–10 µl, 10% sucrose). Go-trials (tactile stimulus) were randomly interleaved with Catch-trials (no tactile stimulus). (**b**) Rate of HIT (green) and false alarm (FA; fawn) trials throughout learning of the tactile-association task (n = 32 mice). Data presented from individual mice (lines) and as mean (circles). (**c**) Discriminability index (d') throughout learning (n = 32 mice). Data presented as individual mice (lines) and mean (circles).

https://doi.org/10.1038/s41593-022-01198-z

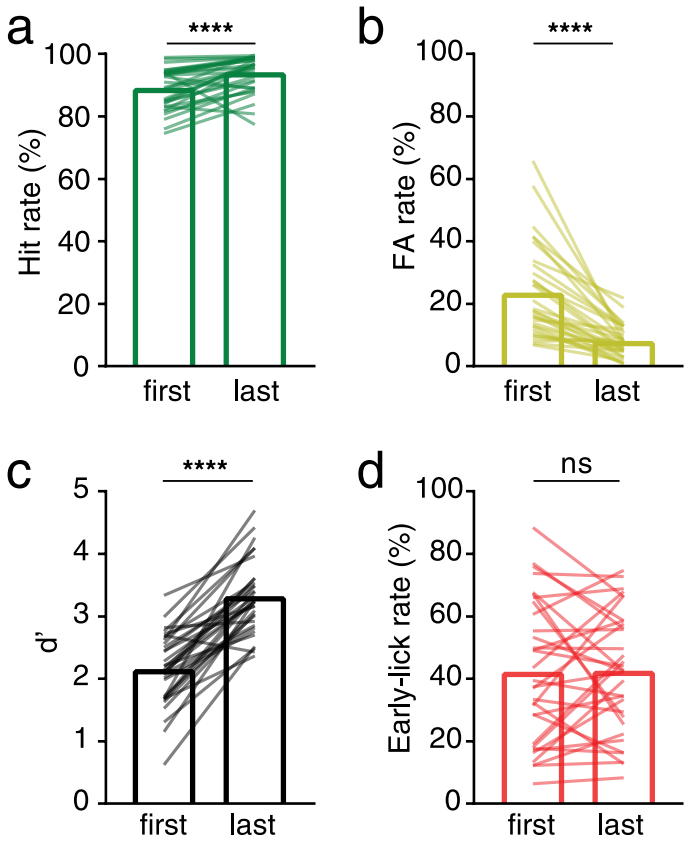

Extended Data Fig. 2 | Improvement in performance during the cued sensory association task following the introduction of an auditory cue. (**a**) HIT (correct), (**b**) False-alarm (FA), (**c**) Discriminability index (d'), and (**d**) Early-lick (EL) rate in the first and last day after introducing the auditory cue during the cued-sensory association task (HIT, $P < 0.0001$; FA, $P < 0.0001$; d', $P < 0.0001$; EL, $P = 0.82$; two tailed Wilcoxon tests, $n = 32$ mice). ns, $P > 0.05$; ****, $P < 0.0001$.

https://doi.org/10.1038/s41593-022-01198-z

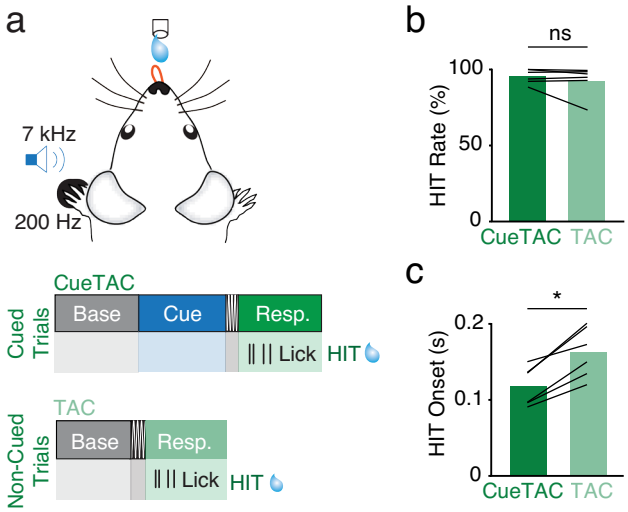

Extended Data Fig. 3 | Performance in the cued-sensory association task during cue omission. (**a**) The cued sensory association task design. Mice were trained to lick a water port within 1 s of a tactile stimulation (200 Hz, 100 ms). Tactile stimulus was presented either in isolation (non-cued trials; TAC) or preceded by an auditory cue (cued trials; CueTAC; 1 s, 7 kHz, 60 dB). Trials were randomly interleaved. (**b**) Rate of HIT during CueTAC and TAC trials ($P = 0.69$, two tailed Wilcoxon test, $n = 6$ mice). Data presented as individual mice (lines) and mean of all mice (bars). (**c**) The average onset of the licking response during CueTAC and TAC trials ($P = 0.03$, two tailed Wilcoxon test, $n = 6$ mice). Data presented as individual mice (lines) and mean of all mice (bars). ns, $P > 0.05$; *, $p < 0.05$.

https://doi.org/10.1038/s41593-022-01198-z

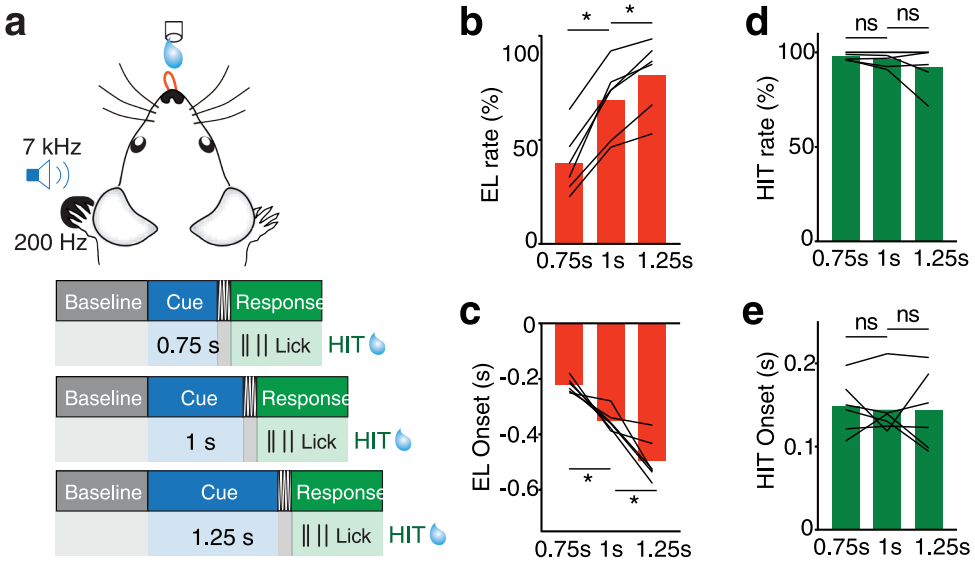

Extended Data Fig. 4 | Performance in the cued sensory association task during variable cue duration. (**a**) The cued sensory association task design. Mice were trained to lick a water port within 1 s of a tactile stimulation (200 Hz, 100 ms). Tactile stimulus was preceded with an auditory cue (7 kHz, 60 dB) with variable duration (0.75 s, 1 s and 1.25 s). (**b**) Rate of EL performance during trials with different cue duration (1 s versus 0.75 s, P = 0.03; 1 s versus 1.25 s, P = 0.03; two tailed Wilcoxon test, n = 6 mice). (**c**) The average onset of the EL licking response during trials with different cue duration (1 s versus 0.75 s, P = 0.03; 1 s versus 1.25 s, P = 0.03; two tailed Wilcoxon test, n = 6 mice). (**d**) Rate of HIT performance during trials with different cue duration (1 s versus 0.75 s, P = 0.25; 1 s versus 1.25 s, P = 0.63; two tailed Wilcoxon test, n = 6 mice). (**e**) The average onset of the HIT licking response during trials with different cue duration (1 s versus 0.75 s, P = 0.99; 1 s versus 1.25 s, P = 0.84; two tailed Wilcoxon test, n = 6 mice). Data presented from individual mice (lines) and as mean (bars). ns, P > 0.05; *, P < 0.05.

https://doi.org/10.1038/s41593-022-01198-z

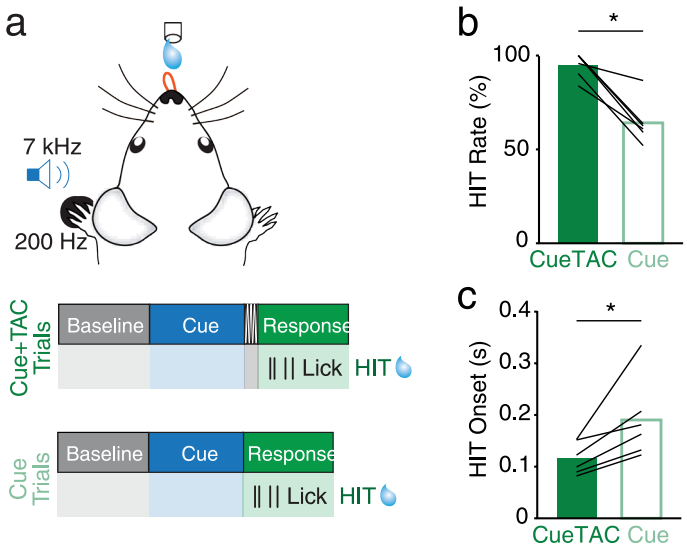

Extended Data Fig. 5 | Performance in the cued sensory association task during omission of the tactile stimulus. (**a**) The cued sensory association task design. Mice were initially trained to lick a water port in response to tactile stimulation (200 Hz, 100 ms) which was preceded by an auditory cue (1 s, 7 kHz, 60 dB; CueTAC). Then, in a subset of randomly interleaved trials, the tactile stimulus was omitted and only the auditory cue was presented to the mouse (Cue). Therefore, mice were presented with either the cue with (CueTAC) or without (Cue) the tactile stimulus. (**b**) HIT rate and (**c**) average onset of the licking response during CueTAC and Cue trials (HIT rate, P = 0.03; HIT Onset, P = 0.03; two tailed Wilcoxon test, n = 6 mice). Data presented as individual mice (lines) and mean of all mice (bars). *, P < 0.05.

https://doi.org/10.1038/s41593-022-01198-z

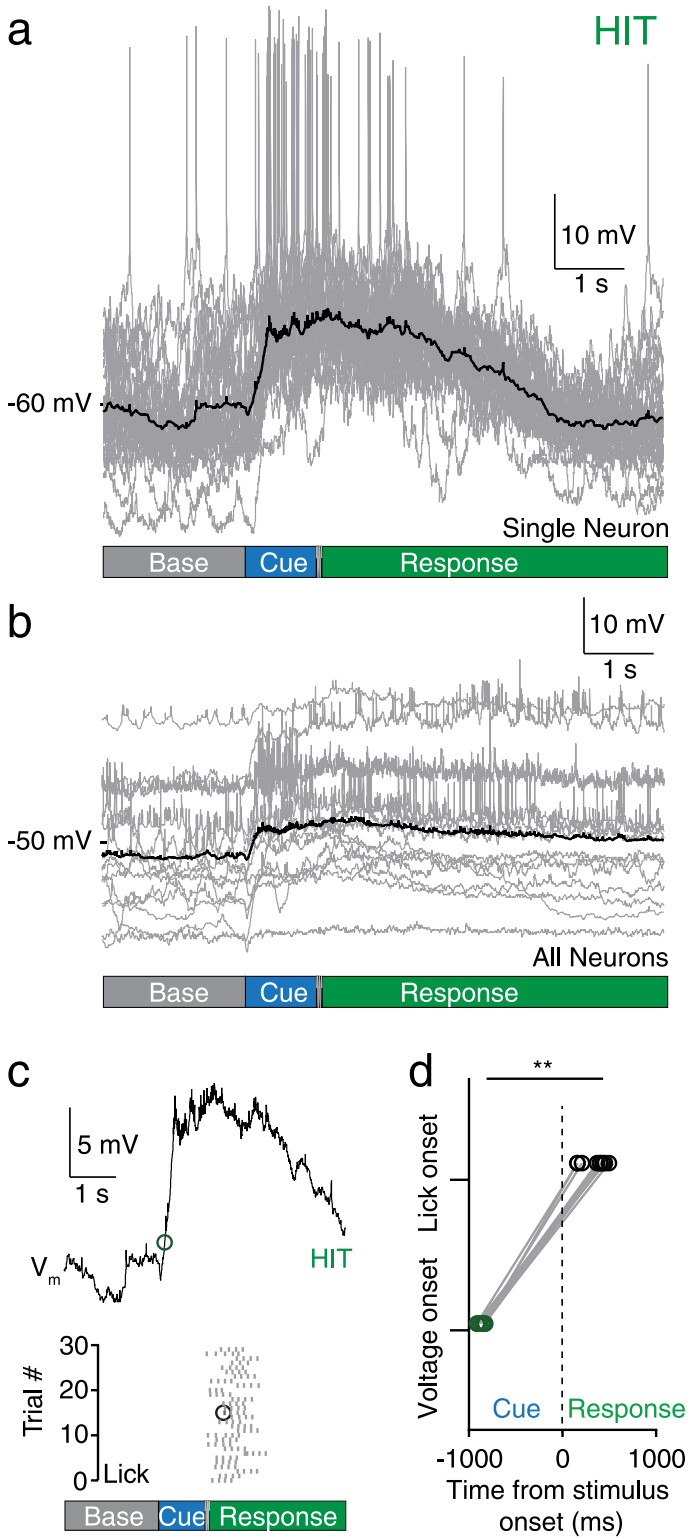

Extended Data Fig. 6 | Voltage response during correct HIT performance in the cued sensory association task and its relation to timing of the licking response. (**a**) Overlay of individual voltage responses during HIT trials (grey) and average of all HIT trials (black) in an example L2/3 pyramidal neuron. (**b**) Overlay of the average voltage responses during HIT trials of individual (grey) and average of all (black) L2/3 pyramidal neurons (n = 11 neurons, 4 mice) during HIT performance (light green) and its average (dark green). (**c**) Average voltage response (top) and licking response (bottom) during all HIT trials in the example L2/3 pyramidal neuron shown in (a). (**d**) Onset of the voltage occured before the first lick in HIT trials (P = 0.004, two tailed Wilcoxon test, n = 9 neurons, 4 mice). **, P < 0.01.

https://doi.org/10.1038/s41593-022-01198-z

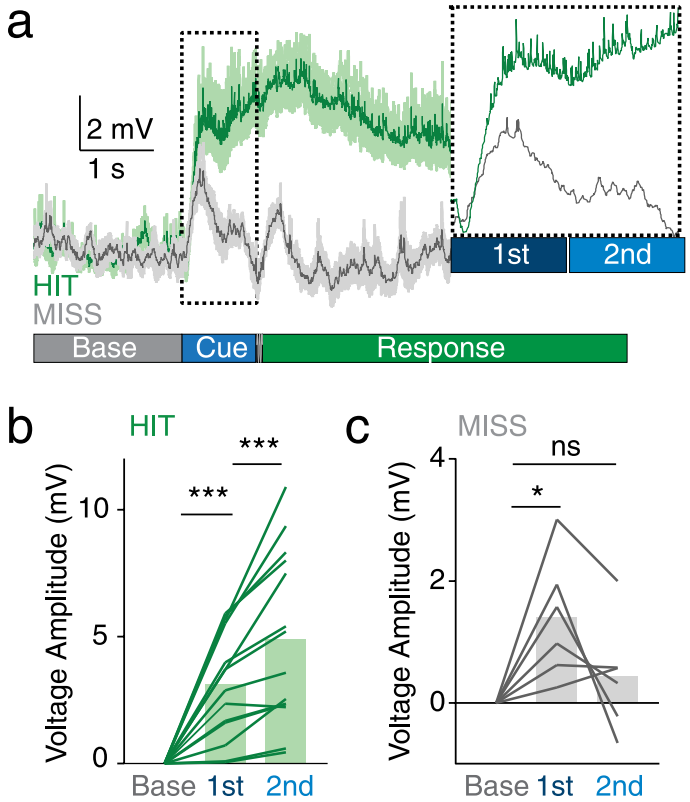

Extended Data Fig. 7 | Voltage responses in ALM neurons during the auditory cue. (**a**) Overlay of the grand average (dark) and sem (light) voltage response for all recorded neurons during HIT (green) and MISS (grey) trials. Insert, zoom of voltage during the auditory cue. Auditory cue separated into 1st (0–500 ms) and 2nd (500–1000 ms) portion. (**b**) Amplitude of the voltage response in HIT trials during the 1st and 2nd portion of the auditory cue compared to baseline (baseline versus 1st portion of the cue, P = 0.0001; baseline versus 2nd portion of the cue, P = 0.0002; two tailed Wilcoxon test, n = 14 neurons, 4 mice). (**c**) Amplitude of the voltage response in MISS trials during the 1st and 2nd portion of the auditory cue compared to baseline (baseline versus 1st portion of the cue, P = 0.03; baseline versus 2nd portion of the cue, P = 0.44; two tailed Wilcoxon test, n = 6 neurons, 4 mice). ns, P > 0.05; *, P < 0.05; ***, P < 0.001.

https://doi.org/10.1038/s41593-022-01198-z

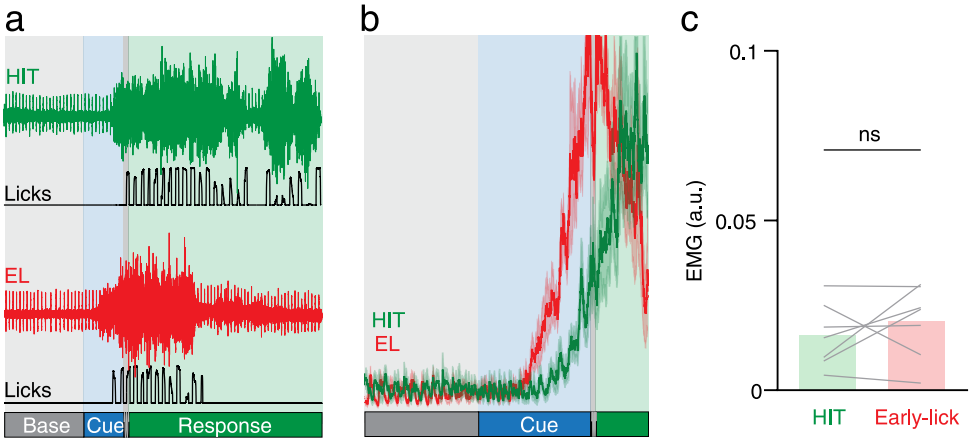

Extended Data Fig. 8 | Nuchal EMG activity during HIT and early-lick trials. (**a**) Example EMG activity during HIT (top) and early-lick (bottom; EL) trials. (**b**) Grand average (dark) and sem (light) EMG activity during HIT (green) and early-lick (red) trials from example in (a). (**c**) Average EMG activity during the beginning of the cue prior to licking responses (0–0.3 s) in HIT and early-lick trials ($P = 0.47$, two tailed Wilcoxon test, $n = 7$ sessions, 3 mice). ns, $P > 0.05$.

https://doi.org/10.1038/s41593-022-01198-z

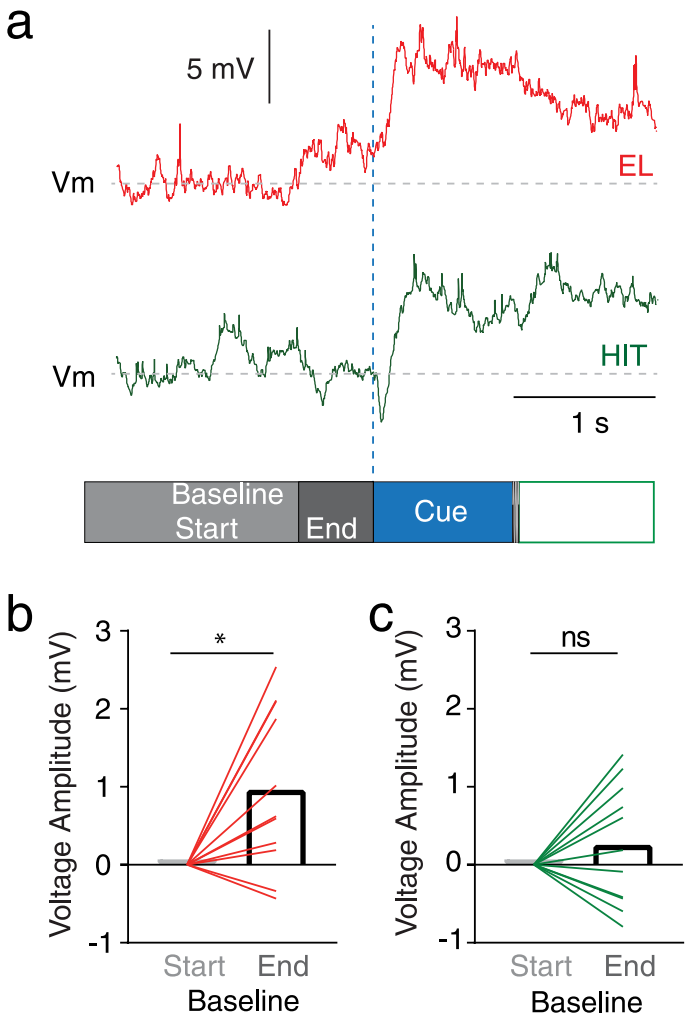

Extended Data Fig. 9 | Ramping baseline during early-lick trials. (**a**) Example voltage responses recorded from a layer 2/3 pyramidal neuron within ALM during early-lick (EL) and correct (HIT) trials. Average baseline voltage at the start (0–1.5 s) and end (1.5–2 s) of the baseline epoch during (**b**) early-lick trials ($P = 0.02$, two tailed Wilcoxon test, $n = 11$ neurons, 4 mice) and (**c**) HIT trials ($P = 0.32$, two tailed Wilcoxon test, $n = 11$ neurons, 4 mice). ns, $P > 0.05$; *, $P < 0.05$.

https://doi.org/10.1038/s41593-022-01198-z

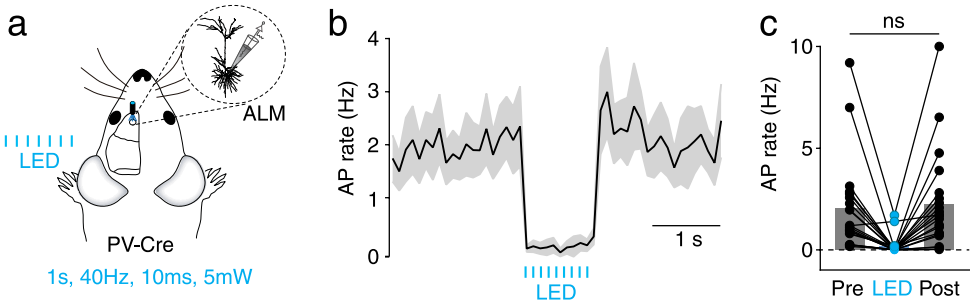

Extended Data Fig. 10 | Firing rates of ALM pyramidal neurons during and after photo-activation of PV interneurons. (**a**) Experimental design. PV^{+} Cre transgenic mice were previously injected with the light sensitive opsin ChR2 (pAAV-EF1a-doublefloxed-hChR2(H134R)-EYFP-WPRE-HGHpA) into the ALM (AP 2.5, ML 1.5 from Bregma). After 2 weeks expression, whole-cell patch-clamp recordings were performed in pyramidal neurons within the ALM during photo-activation of PV interneurons by blue LED pulses (470 nm, 40 Hz, 10 ms, 2–5 mW) delivered to the cortical surface. (**b**) Average (black) and sem (grey) firing rate during ChR2 activation for all recorded ALM neurons (n = 21 neurons, 5 mice). (**c**) Firing rate of ALM pyramidal neurons before, during and after photoactivation of PV interneurons ($P = 0.29$, two tailed Wilcoxon test, n = 21 neurons, 5 mice). ns, $P > 0.05$.

nature portfolio

Corresponding author(s): Robertas Guzulaitis, Lucy M Palmer

Last updated by author(s): Sep 22, 2022

Reporting Summary

Nature Portfolio wishes to improve the reproducibility of the work that we publish. This form provides structure for consistency and transparency in reporting. For further information on Nature Portfolio policies, see our Editorial Policies and the Editorial Policy Checklist.

Statistics

For all statistical analyses, confirm that the following items are present in the figure legend, table legend, main text, or Methods section.

n/a	Confirmed	
☐	☒	The exact sample size (*n*) for each experimental group/condition, given as a discrete number and unit of measurement
☐	☒	A statement on whether measurements were taken from distinct samples or whether the same sample was measured repeatedly
☐	☒	The statistical test(s) used AND whether they are one- or two-sided *Only common tests should be described solely by name; describe more complex techniques in the Methods section.*
☐	☒	A description of all covariates tested
☐	☒	A description of any assumptions or corrections, such as tests of normality and adjustment for multiple comparisons
☐	☒	A full description of the statistical parameters including central tendency (e.g. means) or other basic estimates (e.g. regression coefficient) AND variation (e.g. standard deviation) or associated estimates of uncertainty (e.g. confidence intervals)
☐	☒	For null hypothesis testing, the test statistic (e.g. *F*, *t*, *r*) with confidence intervals, effect sizes, degrees of freedom and *P* value noted *Give P values as exact values whenever suitable.*
☒	☐	For Bayesian analysis, information on the choice of priors and Markov chain Monte Carlo settings
☒	☐	For hierarchical and complex designs, identification of the appropriate level for tests and full reporting of outcomes
☒	☐	Estimates of effect sizes (e.g. Cohen's *d*, Pearson's *r*), indicating how they were calculated

Our web collection on statistics for biologists contains articles on many of the points above.

Software and code

Policy information about availability of computer code

Data collection	Custom-written Igor Pro software (v.6.3, WaveMetrics) was used for the acquisition of whole-cell electrical recordings. Behavior was recorded using Bpod (Sanworks).
Data analysis	Custom-written Igor Pro software (v.6.3, WaveMetrics) was used for the analysis of whole-cell electrical recordings. Changes in pupil diameter were recorded and measured online using a custom software (Pylon-PD, Eridian Systems, Berlin, Germany) kindly provided by Viktor Bahr, Jens Kremkow and Robert Sachdev and colleagues (Bergmann R et al., eNeuro, 2022). Behavior was analyzed using custom written Matlab 2019a codes. Statistical tests were performed using Prism software (v.9, GraphPad).

For manuscripts utilizing custom algorithms or software that are central to the research but not yet described in published literature, software must be made available to editors and reviewers. We strongly encourage code deposition in a community repository (e.g. GitHub). See the Nature Portfolio guidelines for submitting code & software for further information.

Data

Policy information about availability of data

All manuscripts must include a data availability statement. This statement should provide the following information, where applicable:

- Accession codes, unique identifiers, or web links for publicly available datasets
- A description of any restrictions on data availability
- For clinical datasets or third party data, please ensure that the statement adheres to our policy

Data supporting the findings of this study are available within the paper and its Supplementary Information files.

Field-specific reporting

Please select the one below that is the best fit for your research. If you are not sure, read the appropriate sections before making your selection.

☒ Life sciences ☐ Behavioural & social sciences ☐ Ecological, evolutionary & environmental sciences

For a reference copy of the document with all sections, see nature.com/documents/nr-reporting-summary-flat.pdf

Life sciences study design

All studies must disclose on these points even when the disclosure is negative.

Sample size	No statistical method was used to predetermine sample size but our sample size are similar to those reported in previous publications (McGinley M. J. et al 2015, Takahashi N. et al T 2021).
Data exclusions	No data were excluded from the analyses.
Replication	Every finding in the manuscript was shown in multiple mice and therefore replicated across mice.
Randomization	No randomization of mice was done as all mice were trained and recorded under the same conditions. Presentation of different trial types (Go and Catch) was randomized within each training session. There was also a variable delay between trials to randomize the trial start time.
Blinding	Since the analysis procedures were either fully or semi-automated, the Investigators were not blinded to allocation during experiments and outcome assessment.

Reporting for specific materials, systems and methods

We require information from authors about some types of materials, experimental systems and methods used in many studies. Here, indicate whether each material, system or method listed is relevant to your study. If you are not sure if a list item applies to your research, read the appropriate section before selecting a response.

Materials & experimental systems

n/a	Involved in the study
☒	☐ Antibodies
☒	☐ Eukaryotic cell lines
☒	☐ Palaeontology and archaeology
☐	☒ Animals and other organisms
☒	☐ Human research participants
☒	☐ Clinical data
☒	☐ Dual use research of concern

Methods

n/a	Involved in the study
☒	☐ ChIP-seq
☒	☐ Flow cytometry
☒	☐ MRI-based neuroimaging

Animals and other organisms

Policy information about studies involving animals; ARRIVE guidelines recommended for reporting animal research

Laboratory animals	C57BL/6 mice (PN28-60; Australian Resource Centre) and PV-Cre (PN28-60; Jackson Laboratories #008069) female mice were used in this study. Mice were housed in groups of up to six individuals in a 12:12 natural light/dark cycle. Room temperature was kept constant between 18-24 degrees and humidity between 40-70 %.
Wild animals	N/A
Field-collected samples	N/A
Ethics oversight	All procedures were approved by the Florey Institute of Neuroscience and Mental Health Animal Care and Ethics Committee (18-035-FINHMH) and followed the guidelines of the Australian Code of Practice for the Care and Use of Animals for Scientific Purposes.

Note that full information on the approval of the study protocol must also be provided in the manuscript.